
Language Model Evolution: An Iterated Learning Perspective

Yi Ren¹ Shangmin Guo² Linlu Qiu³ Bailin Wang³ Danica J. Sutherland^{1,4}

Abstract

With the widespread adoption of Large Language Models (LLMs), the prevalence of iterative interactions among these models is anticipated to increase. Notably, recent advancements in multi-round self-improving methods allow LLMs to generate new examples for training subsequent models. At the same time, multi-agent LLM systems, involving automated interactions among agents, are also increasing in prominence. Thus, in both short and long terms, LLMs may actively engage in an evolutionary process. We draw parallels between the behavior of LLMs and the evolution of human culture, as the latter has been extensively studied by cognitive scientists for decades. Our approach involves leveraging Iterated Learning (IL), a Bayesian framework that elucidates how subtle biases are magnified during human cultural evolution, to explain some behaviors of LLMs. This paper outlines key characteristics of agents' behavior in the Bayesian-IL framework, including predictions that are supported by experimental verification with various LLMs. This theoretical framework could help to more effectively predict and guide the evolution of LLMs in desired directions. The code is available at <https://github.com/Joshua-Ren/iICL>.

1. Introduction

Recent large language models (LLMs) have shown remarkable instruction-following ability and an increasing number of applications; it is thus reasonable to expect they are likely to become more widespread. Moreover, *interactions* between LLMs (either multiple models, or different generations of the same model) may also become very commonplace in the near future. In fact, many recent works consider iterative self-data-augmentation solutions to break through

the bottleneck of human-generated supervisions, e.g., self-instruct (Wang et al., 2022), self-refine (Madaan et al., 2023), hypothesis refinement (Qiu et al., 2024), self-distill (Xu et al., 2023), self-instruct (Wang et al., 2022), self-reward (Weizhe et al., 2024), self-feedback (Xu et al., 2024), RAFT (Dong et al., 2023), ReST (Gulcehre et al., 2023), iterated DPO (Xiong et al., 2023), OAIF (Guo et al., 2024), SPIN (Chen et al., 2024), and many more. Whether the model's knowledge is updated through in-weight or in-context mechanisms, these methods involve an LLM learning from a corpus (comprising data examples or evaluations) generated by another LLM (or itself), and subsequently transferring this acquired knowledge to others. Looking towards the long term, the future Internet may (for better or worse) contain substantial portions of LLM-generated text, which will, in turn, be employed for training the subsequent generation of models. It thus seems important to begin studying what this process will mean for future models.

Although these self-improving methods demonstrate considerable improvements on various benchmarks, a systematic understanding of why they work and what is their limitations is still missing. Some analysis of knowledge distillation might bring insights (Mobahi et al., 2020), as learning from data generated by another model is a type of distillation. However, as LLMs continue to grow more complex, a precise bottom-up analysis becomes increasingly difficult. Instead, a top-down, behavioral-level analysis might be fruitful, akin to how the Bayesian framework can aid in comprehending the human cognitive system (Griffiths et al., 2023). By conceptualizing the LLM as an intelligent agent, we can draw parallels between its behaviors and the cultural evolution observed in humans. Iterated learning (IL), a framework proposed to study the evolution of knowledge and beliefs through a chain of learning among Bayesian agents (Kirby et al., 2007), stands out as a promising candidate for achieving our goals.

In this paper, we start by introducing the Bayesian-IL framework, demonstrating that agents engaged in such a process gradually amplify bias in their priors. This amplification process can be steered by introducing an interaction phase that “filters” or “re-ranks” the messages generated by the agents. Next, we theoretically justify that the in-context behavior of LLMs can be approximated by a Bayesian update, establishing a crucial link to the LLM system. To validate

¹University of British Columbia, Canada ²University of Edinburgh, UK ³Massachusetts Institute of Technology, USA ⁴Alberta Machine Intelligence Institute, Canada. Correspondence to: Yi Ren <renyi.joshua@gmail.com>, Danica J. Sutherland <dsuth@cs.ubc.ca>.

our claims, we conduct numerous experiments across different settings. Depending on the beneficial or detrimental nature of the bias, we propose various strategies to guide the evolution of LLM. The key contributions of this work are: 1) establishing the first Bayesian analysis of the full interactive learning process (including an interaction phase); 2) applying this framework to LLM agents and describing their evolution theoretically; 3) validating the theory and demonstrating how to guide LLM’s evolution using experiments. We believe that our analysis can enhance our understanding of LLMs, and aid in the design of more effective algorithms for alignment, data filtering, bias mitigation or amplification, and similar tasks.

2. Background and Related Work

2.1. Iterated Learning

Iterated learning (IL) is a hypothetical procedure to simulate how specific properties of human culture or language gradually emerge and become dominant. It is based on studying the behaviors of a chain of intelligent agents. From the perspective of an individual agent, the process involves initially acquiring knowledge from its predecessor (*imitation*), refining its beliefs while using them to conduct tasks (*interaction with the world*), and subsequently imparting its knowledge to the agents in the next generation (*transmission*).

Cognitive scientists and linguists have applied this framework to explain various evolutionary phenomena of human society, including the emergence of compositionality in human language (Kirby et al., 2015), patterns in human object categorisation (Griffiths et al., 2008), and the evolution of color naming systems (Carlsson et al., 2023). The framework has also seen recent success with neural network agents, including in emergent communication (Ren et al., 2020; Guo et al., 2019), machine translation (Lu et al., 2020), visual question answering (Vani et al., 2021), large vision-language models (Chenhao et al., 2024), and representation learning (Ren et al., 2023), indicative that this framework could also be useful for more general AI agents, like LLMs. Appendix C gives a more detailed discussion of IL, but Section 3.2 should be sufficient for our needs.

2.2. Related Self-data-augmentation Methods

While the theoretical guarantees for the Bayesian-IL framework studied in this paper rely on several assumptions, we posit that the behaviors observed for many recent “iterative self-data-augmentation” methods in LLM can be at least partially explained by the theory. We will now overview the basic assumptions, and how they fit with recent LLM approaches (please refer to Appendix A for more discussions).

First, the theory assumes “self-evolution,” where all agents in different generations share the same initial knowledge.

Methods like self-refine (Madaan et al., 2023) and hypothesis refinement (Qiu et al., 2024), which require the LLM to refine its output by the feedback from an identical LLM for several rounds, satisfy this assumption. Self-distill (Xu et al., 2023) and self-instruct (Wang et al., 2022), if the models involved in different generations are the same, do as well. On the contrary, the super-alignment setting (Burns et al., 2023), where a stronger model is trained using the data generated by another weaker model, do not strictly fit with our analysis. However, if all the models are trained using a similar corpus, so that their initial knowledge should be similar, our analysis might still hold.

The theory also assumes the information transferred among agents is in the form of data examples, as in RAFT (Dong et al., 2023) and ReST (Gulcehre et al., 2023). Both methods consider a multi-generation data-transferring process, during which the bias is introduced by re-ranking the transferred data. Methods like self-reward (Weizhe et al., 2024) and self-refine (Madaan et al., 2023), which require one agent to evaluate another agent’s response, do not directly fit this assumption. However, if we also consider the evaluation as part of the data generated by the agent, the Bayesian-IL framework can still bring some insights.

Last, the knowledge update strategy among these methods varies from in-context learning to in-weight learning. We will elaborate on this point in Section 4.2.

2.3. Significance of Explaining Self-evolution of LLM

As mentioned in Section 1, the self-evolution of LLM agents might occur in both the short and long term. Anticipating future trends, we posit that iterative self-data-augmentation methods will likely gain popularity, given their scalability and potential to be a pivotal factor in achieving super-alignment (Burns et al., 2023). It is also foreseeable that the future Internet will contain increasing amounts of data generated by AI, much of which will likely train the next-generation model. Therefore, we contend that a theoretical framework for self-evolution not only enhances our comprehension of the strengths and limitations of current methods but also offers insights into guiding the long-term evolution of LLMs. While acknowledging that the proposed theory may only give some rough insight into the evolution of future AI agents, it may help in developing guiding principles for steering LLM evolution toward alignment and safety. This work hopes to be one of many steps toward realizing this ambitious vision.

3. Bayesian Analysis of Iterated Learning

3.1. Notations and Basic Behaviors

We denote a data pair as $d = (x, y)$, where $d \in \mathcal{D} = \mathcal{X} \times \mathcal{Y}$, with $x \in \mathcal{X}$ and $y \in \mathcal{Y}$. The (x, y) pair can be question and

answer in a QA problem, the input and label in a supervised setting, or any type of prompt and output for in-context learning. The hypothesis $h \in \mathcal{H} : \mathcal{X} \rightarrow \mathcal{Y}$ describes the mapping between all possible x and their corresponding y . Note that h can be either explicit or implicit, depending on the task. For instance, in inductive reasoning, h represents the rule determining the output from input examples and is explicit, as the model can directly generate it using natural language. Conversely, in self-data-augmentation, where x is a topic and y is a paragraph generated based on x , h is likely to be implicit. In this context, h can be highly abstract with varying interpretations, such as the level of conciseness, helpfulness, or even the writer’s preference for using rhyme. Further discussion on this will be provided later.

Consider a general Bayesian agent whose behavior can be depicted by two basic procedures: *learning* and *sampling*. Learning involves updating the agent’s knowledge based on observations, while sampling is a procedure wherein the agent generates data based on its knowledge. In this context, the agent’s knowledge is encapsulated by its posterior over the hypotheses, i.e., $P_{lm}(h)$.¹

In learning, we assume the agent holds a prior $P_0(h)$ before learning. Its posterior after observing $\mathbf{d} = (x_i, y_i)_{i=1}^N$ is calculated as

$$P_{lm}(h) = P(h \mid \mathbf{d}) \propto p(\mathbf{d} \mid h) \cdot P_0(h), \quad (1)$$

where $p(\mathbf{d} \mid h)$ is the likelihood of these N data pairs under a specific h ; this is usually hard to calculate in practice.

Assume the agent holds a posterior $P_{lm}(h)$ during sampling. Then, given the input signal x , we can sample the corresponding $y \sim P_{lm}(y \mid x)$. Based on the fact that h determines the relationship between x and y , the above sampling procedure is equivalent to $y \sim \mathbb{E}_{h \sim P_{lm}(h)}[p(y \mid h, x)]$, which can be rewritten as $h \sim P_{lm}(h)$; $y \mid h \sim p(y \mid h, x)$. Following the definition of d and the assumption that x is uniformly distributed, the sampling procedure above is equivalent to $d \sim P_{lm}(d) \propto p(d \mid h) \cdot P_{lm}(h)$. If we instead first decide the most probable h rather than sampling h from the agent (maximum a posteriori (MAP), as is perhaps common subconscious behavior for humans), we then generate d by

$$d \sim p(d \mid h^*), \quad h^* = \underset{h}{\operatorname{argmax}} P_{lm}(h). \quad (2)$$

3.2. Iterated Learning of Bayesian Agents

Iterated learning is a hypothetical process simulating how human language gradually evolves to become more efficient when transferred and utilized across generations. Typically, iterated learning repeats of the following three phases, as

¹The agent is not necessarily a language model, but we call the posterior $P_{lm}(h)$ for convenience.

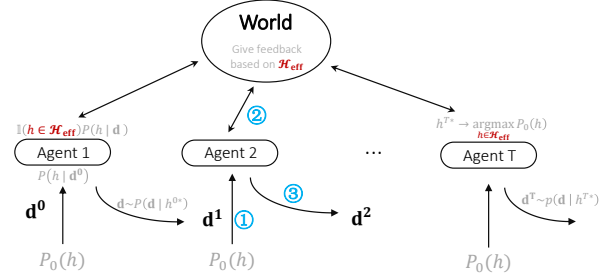


Figure 1: Typical iterated learning, where ①, ②, and ③ denotes the imitation, interaction and transmission phases. Some early works (e.g. Griffiths & Kalish, 2007) on iterated learning only consider ① and ③. We will extend the theory by introducing the interaction phase.

illustrated in Figure 1: an *imitation phase*, where an ignorant agent learns from the data generated by its predecessor; an *interaction phase*, where this agent uses the knowledge to accomplish the task, and hence refine its knowledge; and a *transmission phase*, where this agent generates useful data for the next generation. Combining with Section 3.1, we can get a picture of how h and d evolve as follows.

Initialization: at the beginning of the t th generation, a new agent $_t$, whose belief on h follows a prior distribution $P_0(h)$, is initialized. In lab experiments, $P_0(h)$ represents the belief of a well-educated participant who has not been previously involved in the target experiment. In in-context learning, a well-trained LLM also holds a complex and informative $P_0(h)$ based on the enormous corpus it is trained on and the task instructions in the prompt.

Imitation phase: after initialization, agent $_t$ then updates its knowledge by observing N data samples \mathbf{d}^{t-1} . Following the learning procedure defined in Equation (1), the model’s posterior should be $P(h \mid \mathbf{d}^{t-1})$.

Interaction phase: in this phase, the agent will accomplish specific tasks to refine its knowledge. The tasks involved in this phase can be diverse and complex. For example, in lab experiments (Kirby et al., 2015) and emergent communication (Ren et al., 2020), the agent plays a Lewis referential game (Lewis, 2008) to rule out hypotheses representing a non-bijection between \mathcal{X} and \mathcal{Y} ; in representation learning (Ren et al., 2023), the agent directly conducts supervised learning on the downstream task to inhibit insufficient representations. Although it is hard to precisely formalize the behavior of the agent under these tasks precisely, their goals are consistent: we expect to “rule out” unsuitable hypotheses with carefully designed interactions. In an idealized setting, we might expect the agent’s posterior to become proportional to $\mathbb{1}(h \in \mathcal{H}_{\text{eff}})P(h \mid \mathbf{d}^{t-1})$, where $\mathbb{1}(\cdot)$ is an indicator function and $\mathcal{H}_{\text{eff}} \subset \mathcal{H}$ is the subset of hypotheses that can accomplish the tasks. Broadly speaking, refining h or filtering \mathbf{d}^t using the feedback from humans, LLM, or

the environment, which is common in the aforementioned iterative self-data-augmentation methods, is also a type of task implicitly constraining $h \in \mathcal{H}_{\text{eff}}$.

Transmission phase: agent _{t} now comes to the transmission phase, where it generates multiple data samples \mathbf{d}^t for the next generation. The agent will first select the most probable hypothesis based on its current belief and then generate data samples, i.e., $d_i^t \sim p(d \mid h^{t*})$, where $h^{t*} = \operatorname{argmax}_{h \in \mathcal{H}_{\text{eff}}} P(h \mid \mathbf{d}^{t-1})$. This accomplishes one generation of iterated learning.

3.3. The Limiting Behavior

In iterated learning, we repeat the phases mentioned above to get better h and \mathbf{d} . The limiting behavior of this process can be described by the following proposition:

Proposition 1. *Consider several Bayesian agents sharing the same prior $P_0(h)$ are conducting iterated learning for T generations. If T is sufficiently large, then no matter the choice of \mathbf{d}^0 , any agent _{t} with $t > T$ will have*

$$P_{lm}(h) \rightarrow \mathbb{1}(h = h^{T*})$$

where h^{T*} is a stationary point (e.g. a local maximum) of $P_0(h)$ subject to $h \in \mathcal{H}_{\text{eff}}$.

To prove this, we first analyze iterated learning without the interaction phase. By drawing parallels between IL and EM (expectation-maximization) algorithms, we can prove that h^{T*} converges to the h with the maximum prior probability. We then consider the interaction phase, which introduces a ‘‘selection’’ pressure to rule out those $h \notin \mathcal{H}_{\text{eff}}$. By proving this process does not break the converging behavior of a non-interacting iterated learning, we achieve this proposition. (Please refer to Appendix B for more details.)

Based on this proposition, we conclude the following three important behaviors of the Bayesian-IL chain:

- For convex target, the converged h^{T*} only depends on $P_0(h)$ and \mathcal{H}_{eff} , which is irrelevant to the selection of \mathbf{d}^0 . A good \mathbf{d}^0 , however, leads to a faster convergence.
- The biases in $P_0(h)$ are amplified during learning, which also reduces the entropy of $P_{lm}(h)$.
- Carefully designed interaction phase introduces appropriate \mathcal{H}_{eff} , and hence restrains harmful h .

These behaviors can be precisely verified by experiments on Bayesian agents in an experiment on compositional mapping (see Appendix C.2). In the next section, we will link the analysis to the LLM agents and demonstrate what iterated learning brings to the evolution of LLM agents.

4. LLM-based Agents in Iterated Learning

4.1. LLM as Bayesian Agents

To transfer the Bayesian-IL analysis to LLM, we first show that the learning and sampling behaviors of an LLM agent can be depicted by Bayesian inference. Following the setting of Xie et al. (2022), we also consider a few-shot in-context learning (ICL) scenario, where all the examples are composed of the input x followed by the output y . Thus the message feed to the agent would be an instruction prompt \mathbf{w} followed by N examples, i.e., $\mathbf{d}_N = (x_i, y_i)_{i=1}^N$. In other words, sampling y given the prompt, the examples, and the question x_{test} can be represented as:

$$y \sim P_{lm}(y \mid x_{\text{test}}, \mathbf{d}_N, \mathbf{w}) \triangleq P_{lmw}(y \mid x_{\text{test}}, \mathbf{d}_N), \quad (3)$$

where P_{lmw} is the model’s belief conditioned on the instruction \mathbf{w} . If we call \mathbf{d}_N as \mathbf{d}^{t-1} (i.e., assume the examples are generated by agents in the previous generation) and assume the test question x_{test} is uniformly distributed, sampling new data based on instruction and few-shot examples can be expressed as $d^t \sim P_{lmw}(d \mid \mathbf{d}^{t-1})$, which is similar to the transmission phase in iterated learning.

Formally linking ICL and Bayesian-IL poses a non-trivial challenge, however, because the theoretical guarantee of Bayesian-IL relies on obtaining the MAP estimate of h at each generation. This is not immediately evident in the definition of ICL. Inspired by Xie et al. (2022), we first demarginalize this posterior predictive distribution using the latent variable h , and then achieve the following proposition:

Proposition 2. *Consider that agent A is conducting in-context learning. If the prompt examples in \mathbf{d}^{t-1} are generated by another agent B with the same prior knowledge (e.g., they come from the same checkpoint and use the same prompt), sampling from the posterior predictive distribution of agent A, i.e., $d^t \sim P_{lmw}(d \mid \mathbf{d}^{t-1})$, can be decomposed into: 1.) $h^{t*} \rightarrow \operatorname{argmax}_h P_{lmw}(h \mid \mathbf{d}^{t-1})$, and 2.) $d^t \sim P_{lmw}(d \mid h^{t*})$, where h is a hidden variable that describes the mapping between x and y .*

The proof is in Appendix B.3.

4.2. Why we Focus on the In-Context Behavior

In this paper, we consider the in-context behavior of LLM for both sampling and learning. For sampling, we notice that in-context sampling is ubiquitous when the LLM interacts with another agent (e.g., the human, the internal block of an LLM agent, or even the environment), irrespective of the subsequent information-updating strategy. It’s worth noting that the iterative self-data-augmentation methods also require a few-shot example-generating process.

For learning, while an LLM can acquire new knowledge in different ways, e.g., pretraining, supervised fine-tuning,

RLHF, direct preference optimization, etc., we start from the in-context learning for the following reasons.

First, our current theory requires the agents in different generations to share the same prior, which means the instruction prompts \mathbf{w} and the model’s parameters should remain constant during evolution. Second, the multi-round ICL is also common when users interact with private LLMs like ChatGPT, or in a sandbox multi-agent scenario discussed by Park et al. (2023). The LLMs in these scenarios hold a constant $P_0(h)$ because the model parameters are fixed.

However, our framework also has the potential to be extended to the in-weight learning cases. Take those self-improving methods mentioned above as examples, where their sampling phase is identical to ICL. During in-weight learning, the model will pursue a lower loss on the training data \mathbf{d}^{t-1} , which is equivalent to improving the likelihood of $p(\mathbf{d}^{t-1} | h)$ under related h . In other words, this learning improves the probability of h that explains \mathbf{d}^{t-1} by increasing likelihood, which is similar to Bayesian learning to some extent. As the parameters of the models are updated in this process, the $P_0(h)$ of agents in different generations are no longer identical, which violates our assumptions. However, as this knowledge update also reinforces the model’s belief on \mathbf{d}^{t-1} , we speculate that iterative learning with in-weight updates converges faster than the ICL version, as $P_0(h)$ also participates in the evolution. Thus although lacking a theoretical expression of in-weight learning, we believe the Bayesian-IL framework still provides some insights into the success and potential limits of these algorithms. We left the discussion of IL and in-weight learning in our future work.

4.3. Hallmarks of LLM’s Evolution

This subsection will elaborate on what are the benefits and risks for the LLM system if the model evolves in an evolutionary chain that can be depicted by iterated learning.

Selection of \mathbf{d}^0 influences the converging speed, but not the converged value. Proposition 1 claims that the converged h^{T^*} is determined by $P_0(h)$ and \mathcal{H}_{eff} , which is independent of \mathbf{d}^0 . Ideally, h^{T^*} can always be achieved although we start from random or even wrong \mathbf{d}^0 , as illustrated in Figure 9 where the compositional language finally dominates the posterior even if we start from a degenerate language. On another extreme, if we start from a perfect $\mathbf{d}^0 \sim p(\mathbf{d} | h^{T^*})$, then the posterior will converge very fast.

This property proves advantageous, especially considering that practical algorithms often commence with a small set of human-collected \mathbf{d}^0 , which may inherently contain bias or errors. The iterated learning procedure offers a notable benefit: the continual generation of new data pairs through sampling from agents and subsequent filtering during interaction. Essentially, with a sufficiently diverse sampler on x

and a powerful evaluator to constrain h , the limitation posed by the number of labeled data diminishes, explaining the popularity of self-data-augmentation.

However, it is crucial to note that the converging behavior relies on numerous assumptions (akin to those employed in the EM algorithm), which might be violated in practical scenarios. Consequently, there’s a possibility of the evolutionary process getting trapped in local optima. Thus, selecting appropriate \mathbf{d}^0 becomes more important when the convergence guarantees no longer holds.

Amplifying bias in prior is a double-edged sword. As mentioned in Proposition 1, the subtle bias in $P_0(h)$ will be amplified during evolution. If this bias is beneficial, like the simplicity bias in compositional language experiments, IL will help the model generate the “correct messages” more robustly. Imagine if we only have two possible hypotheses, i.e., h_{good} and h_{bad} , where $P_0(h_{\text{good}})$ is slightly larger than $P_0(h_{\text{bad}})$. Then by sampling $y \sim p(y | h, x) \cdot P_0(h)$, half of the chance we will get incorrect y coming from h_{bad} . Although we can get $y = \text{argmax}_y p(y | h, x) \cdot P_0(h)$ by using an extremely small temperature, the diversity of y provided by the likelihood will then disappear, which is not what we expected. How could we get samples that are both diverse and correct? Iterated learning can help with this problem by providing a posterior where $P_{lmw}(h_{\text{good}}) \gg P_{lmw}(h_{\text{bad}})$. With this posterior, sampling from $p(y | h, x) \cdot P_{lmw}(h)$ would be similar to sampling from $p(y | h_{\text{good}}, x)$.

However, amplifying bias in prior can also harm the system in several ways. The first one is the mode collapse of the hypothesis. Imagine we have multiple good h where $P_0(h_{\text{good1}}) > P_0(h_{\text{good2}}) > P_0(h_{\text{bad}})$, then iterated learning will let us lose h_{good2} even its prior is only slightly smaller than h_{good1} . Such a mode decay phenomenon is quite similar to the “recursion curse” mentioned in Shumailov et al. (2023): a more peaky $P_{lmw}(h)$ will make those non-dominating h have a smaller probability, hence it is harder to keep these modalities during evolution. Authors of Touvron et al. (2023) also mentioned that iteratively fine-tuning will harm the creativity of the model. The solution could be early stopping the iterated learning or manually introducing more y that comes from h_{good2} during imitation.

Another problem is that iterated learning can also amplify the malicious bias. To mitigate this, we need a carefully designed interaction phase to put constraints on h . If h is explicit, like in the inductive reasoning problem where the LLM generates hidden rules based on observations, we can explicitly refine $h \in \mathcal{H}_{\text{eff}}$ using self-refine (Madaan et al., 2023) or hypothesis-refine (Qiu et al., 2024), as illustrated in experiments in Section 5. If h is implicit, the constraints can be introduced by restraining d in this phase, like what we do in Section 6. The data-ranking design in RAFT (Dong et al., 2023) and ReST (Gulcehre et al., 2023) also

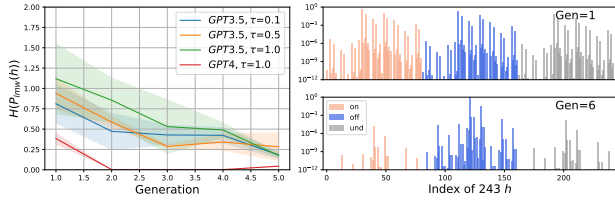


Figure 2: Left: We run five experiments with different h^* and \mathbf{d}^0 and draw the mean and standard deviations of $H(P_{lmw}(h))$ in this panel. Right: the histogram of all $P_{lmw}(h)$ in different generations. We color h with different values of the last object differently. The y-axis is in log-scale and the upper limit of the panel is $P(h) = 1$.

fits in this scenario. Please also refer to the experiment in Appendix C.2 to get a better understanding of this case.

In summary, a carefully designed interaction phase and a good $P_0(h)$ are crucial for agents to evolve as expected.

5. Experiments on Explicit h Case

Section 3 shows that the evolution of Bayesian agents in iterated learning can be well depicted by Proposition 1. Section 4 further claims that the behavior of LLM agents can be explained via Bayes inference, which bridges Bayesian-IL to LLM. This section will verify this claim by experiments on GPT3.5, GPT4, Claude3-haiku, and Mixtral-8x7b under an inductive reasoning task. In this task, h is explicit, as the model needs to infer a rule by observing several input-output pairs, which in turn makes it possible to generate more examples based on this rule.

5.1. Experiment Settings: the ACRE Task

We consider Abstract Causal REasoning (Zhang et al., 2021, ACRE), which is also studied in Qiu et al. (2024). Assume there are M different objects, say $[A, B, C]$. The input x is a list of a subset of these objects. The output y represents the status of the light (could be on, off, or undetermined), which is determined by applying the rule h on x , i.e., $y = h(x)$. In this experiment, the existence of a specific object will trigger the light to be on. The roles played by different objects are determined by the so-called “rule” h . For example, assume $h = \{A:\text{on}, B:\text{off}, C:\text{undetermined}\}$, which means A can trigger the light to be on, B cannot, and C is not sure. In other words, we have $h([A, B, C]) = \text{on}$; $h([B]) = \text{off}$; $h([B, C]) = \text{undetermined}$. The inductive reasoning task requires the model to recover a hidden ground truth h^* from several observations \mathbf{d}^0 . The detailed prompting design related to this experiment can be found in Appendix D.3.

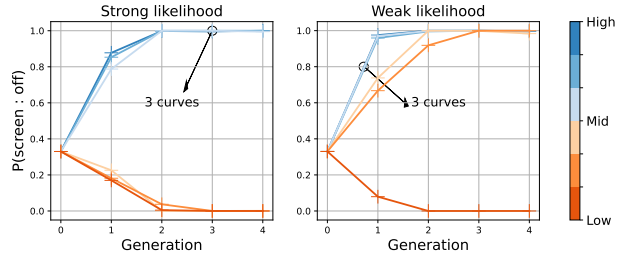


Figure 3: The probability of screen being off. We assume that the model has no preference for these three statuses before seeing the prompt instruction, so all curves start from $\frac{1}{3}$ at generation-0. Different colors represent different levels of spurious bias (full results in Figure 13 and 14).

5.2. Behavior of LLM in Iterated Learning

Convergence of the posterior. We start from the guarantees mentioned in Proposition 1 under an *imitation-only* setting. In this experiment, we choose $M = 5$ to better illustrate the posterior distribution $P_{lmw}(h)$ (there are $3^5 = 243$ possible h under this setting). Thanks to the instruction-following ability, GPT3.5 will always return rules in the correct format, where the probabilities of all format-related tokens are almost one. Thus, we can calculate $P_{lmw}(h)$ or $P_{lmw}(h | \mathbf{d})$ by multiplying the probabilities of specific tokens in their response (see Appendix D.1 for more details).

We first demonstrate the convergence of $P_{lmw}(h)$, i.e., $P_{lmw}(h) \rightarrow \mathbb{1}(\cdot)$, which can be supported by the decreasing of the entropy of the posterior, i.e., $H(P_{lmw}(h))$. As illustrated in the left panel in Figure 2, $H(P_{lmw}(h))$ gradually decreases to a very small value as iterated learning goes on, which verifies our theory that $P_{lmw}(h)$ will converge to a one-hot-like distribution². Smaller temperature τ makes the convergence faster, which matches our intuitions as well. To better illustrate how different h evolves during iterated learning, similar to what we did for the compositional language experiment in Appendix C.2, we also provide the probability of all possible $h \in \mathcal{H}$ in a similar fashion. Note that for this problem, it is impossible to get the prior distribution $P_0(h)$, because we must give the model at least one example as \mathbf{d}^0 . So in the right two panels in Figure 2, we compare the posterior of the first and the sixth generations and see that the posterior becomes sparser.

Converged h under different likelihood and priors. We then show how iterated learning amplifies specific biases implied in the prior, i.e., $h^{T^*} \rightarrow \arg\max_h P_0(h)$, and how the bias and likelihood influence the converging behavior. Note that $P_0(h)$ represents LLM’s belief given the instruction prompt \mathbf{w} , where the few-shot examples are not included. Thanks to the phenomenon mentioned in McCoy et al.

²Note that the entropy of a uniformly distributed h and a one-hot h are roughly 5.34 and 0, respectively.

Table 1: Results when adding different interaction phases. Column "BOTH" represents the ratio of converged h^T (average of the last two generations) who correctly predict all 8 examples in \mathbf{d}^0 and have `screen:off` (i.e., $r_{20}=\text{off}$). The Mixtral model does not have self-refine results, as it often violates the instructions. (10 different seeds)

	Old GPT3.5-Turbo 1106			New GPT3.5-Turbo 0125			Claude3-haiku-20240307			Mixtral-8x7b		
	Corr. \mathbf{d}^0	$r_{20} = \text{off}$	BOTH	Corr. \mathbf{d}^0	$r_{20} = \text{off}$	BOTH	Corr. \mathbf{d}^0	$r_{20} = \text{off}$	BOTH	Corr. \mathbf{d}^0	$r_{20} = \text{off}$	BOTH
imitation-only	4.8±1.56	70%	15%	5.6±1.11	80%	0%	6.4±1.50	90%	30%	5.5±2.01	20%	10%
w. self-refine	7.0±0.60	40%	20%	6.6±1.11	95%	35%	7.0±0.70	60%	15%	-	-	-
w. hypo-search	7.7±0.21	80%	45%	7.4±0.66	100%	55%	7.5±0.67	90%	50%	6.5±1.97	30%	30%

(2023), where the output of LLM is heavily influenced by its degree of familiarity with the output phrases, we can manipulate the prompt to create spurious correlations and hence implicitly control bias in $P_0(h)$. Specifically, we change the name of the last object from “E” to “screen” and add a sentence like “Turn off the screen after the experiment.” in the instruction prompt. Then all h with `screen:off` would have higher prior under this prompt. We use six different prompts to introduce different levels of biases (see Appendix D.2 for more details).

We then control the strength of the likelihood by selecting different h^* . For the strong likelihood case, we select h^* where four objects are being on while there is only one in the weak likelihood case. The status of `screen` in both cases is undetermined. Due to the nature of the ACRE task, i.e., the existence of an on-object in the input will trigger the light on, there might be more examples whose outputs are on when the likelihood is strong. Then it is harder for the model to amplify the prior bias that favors the status of `screen` to be off. Because the likelihood and prior compete with each other during iterated learning, as illustrated by Equation (1).

This competing relationship can be well depicted by Figure 3, 13, and 14. In these figures, we track the probability of $P_{lmw}(\text{screen:off})$ at the end of each generation. The converging speed under different settings correlates with the level of prior bias well. Furthermore, we find it is easier for the bias to be amplified when the likelihood is weaker, as five out of six curves converge to one in the right panel. This trend is more clear in Figure 13 and 14, where curves with the same level of bias are shown together. These results give us a good picture of how the likelihood and prior bias interact with each other during evolution and also verify the correctness of the Bayesian-IL framework for LLM agents. Plus, we plot the histograms of $P_{lmw}(h)$ under weak-likelihood-high-bias case in the right two panels in Figure 3, which also demonstrates the amplified bias.

Interaction phase and \mathcal{H}_{eff} . Finally, we introduce the interaction phase and show that $h^{T^*} \rightarrow \text{argmax}_{h \in \mathcal{H}_{\text{eff}}} P_0(h)$. Two mechanisms are considered in this experiment: self-refine (Madaan et al., 2023), where the feedback comes from the model’s own response; and hypothesis-search (Qiu et al., 2024), where the feedback comes from an external ground-truth interpreter. We can consider the self-refine as

using an *imperfect* \mathcal{H}_{eff} . In both settings, the LLM refines its proposed h^t at the end of each generation by checking whether this h^t can explain all samples in \mathbf{d}^0 .

In this experiment, we give the model 8 different examples in \mathbf{d}^0 , where all these examples can be explained by both h^* and \hat{h} . We first select an \hat{h} from all 162 candidates³ and then create h^* by changing the value of `screen` to `off`. Under this setting, both h^* and \hat{h} belong to \mathcal{H}_{eff} (i.e., mappings with perfect training accuracy in \mathbf{d}^0) and h^* is what we want our model to converge to⁴. See Table 1, where we run experiments under 10 different h^* and report three quantitative metrics of the last iteration, i.e., h^{T^*} . We first report the number of correct predictions (mean and standard error) in \mathbf{d}^0 , which demonstrates how well the method constrains $h^{T^*} \in \mathcal{H}_{\text{eff}}$. The imitation-only method performs the worst, which warns us if the LLM keeps learning from the corpus generated by the agents in previous generations without any evaluation or filtering, even the training accuracy on given \mathbf{d}^0 would be harmed. Because hallucination or incorrectness can aggregate through generations. Adding the interaction phase can mitigate this problem efficiently, which is why most of the related works contain a “data-selection” or “data-reranking” phase. The fact that the hypo-search outperforms self-refine indicates the importance of an appropriate \mathcal{H}_{eff} , which means a good reward (or evaluating) model is crucial for these iterated training methods. Another metric is the ratio of h^{T^*} with `screen:off`, which measures how well the bias is amplified. We find all these methods can amplify the bias to some extent and hypo-search also performs the best. Last, combined with the requirement of good training accuracy and amplifying bias, we report the ratio that the algorithm successfully chose $h^{T^*} = h^*$. As illustrated in the last column of the table, adding an interaction phase with good \mathcal{H}_{eff} always brings benefits.

In summary, this section verifies the correctness of the proposed analysis in LLM agents when the hypothesis is observable. The results remind us to pay more attention to whether the bias is beneficial or not and to design a better interaction phase as well. We would consider another practical scenario when h is hidden in the next section.

³It is $3^4 \times 2$, where the value of `screen` cannot be `off`.

⁴We can draw parallelism with the compositional language experiment in Appendix C.2, where h^* represents compositional mapping, $h^* \cup \hat{h} = \mathcal{H}_{\text{eff}}$ is the space of unambiguous mappings.

6. Experiments on Implicit h Case

Section 5 demonstrates that the Bayesian-IL framework can predict the behavior of LLM agents when h is explicitly defined and utilized when generating new examples. This section considers another general scenario when h is hidden. We consider a few-shot self-data-augmentation task, where the LLM keeps generating new examples to augment the data pool. In this process, h is implicitly selected when the few-shot examples are given, as stated in Proposition 2.

Experiment setting. We choose a scenario where self-data-augmentation is repeated for several generations. Although considering in-weight learning during the imitation phase is more common in recent works (we would extend our analysis to this scenario in our future work), the in-context learning experiment can still demonstrate some crucial trends, because they both require the LLM to generate samples in an in-context way, which matches our analysis well.

Consider using an LLM to generate multiple examples of an acronym-brainstorm task, where each example d is composed of an acronym and the corresponding word list, e.g., Acronym:IL; List:["infinite", "loop"]. As the model generates the acronym-list pair together, it is more convenient for us to treat them as d rather than (x, y) pair. The h determines the properties of d . We hold a data pool $\mathcal{D}_{\text{pool}}$, which contains 20 random samples as \mathbf{d}^0 at the beginning of the experiment. In each generation, the model will generate 20 extra examples based on the data generated by itself in the previous round, i.e., $\mathbf{d}^t \sim P_{lmw}(\mathbf{d} | \mathbf{d}^{t-1})$. The generated \mathbf{d}^t will be pushed into $\mathcal{D}_{\text{pool}}$, which simulates a scenario in which the available data keeps growing when we conduct self-data augmentation.

In this experiment, h is hidden and might have different interpretations. We consider that h represents two types of acronyms, i.e., h_{easy} , where the acronym is a common word, and h_{hard} otherwise. As the training data of GPT3.5 is private, we instead use the ranking of the frequency of a word that appeared in the English corpus⁵ as an approximation. We categorize a word as “easy” if its ranking is below 60,000; otherwise, we label it as “hard”.

Bias in prior is amplified during IL. Many recent works observe that the LLM prefers to output more common words (i.e., those with higher frequency in the pertaining corpus). This can be considered as a bias towards h_{easy} , i.e., $P_0(h_{\text{easy}}) > P_0(h_{\text{hard}})$. However, as h is hidden, we instead track three quantities: 1.) the proportion of easy samples in all 20 samples for each \mathbf{d}^t ; 2.) the average ranking of \mathbf{d}^t (all hard examples are ranked 60,001); and 3.) the average length of the acronyms for \mathbf{d}^t . As in Figure 4, the aforementioned bias is gradually amplified during iterated learning

⁵The frequency and ranking comes from Corpus of Contemporary American English (COCA) (Davies, 2008).

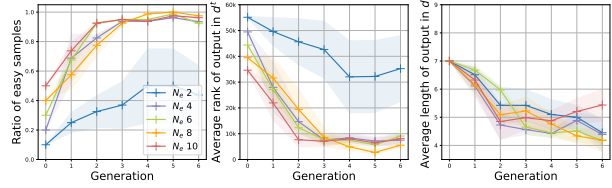


Figure 4: The imitation-only setting. Left: how the ratio of samples coming from h_{easy} changes in each \mathbf{d}^t . N_e is the number of easy examples in \mathbf{d}^0 . Middle: how the average ranking of acronyms in \mathbf{d}^t changes. Right: how the average length of acronyms in \mathbf{d}^t changes. We use 5 different seeds to random sample \mathbf{d}^0 in each setting. The shadow region represents the variance.

whatever the initial proportion of the easy samples in \mathbf{d}^0 is.

Interaction phase when h is hidden. As h is inaccessible, we instead add a filter on the transmitted data across different generations, which plays a similar role as the interaction phase mentioned in the previous section. Specifically, we use a sampled $\mathbf{d} \sim \mathcal{D}_{\text{pool}}(d | h \in \mathcal{H}_{\text{eff}})$ to replace original \mathbf{d}^{t-1} in the “imitation-only” setting. Based on how we sample $\hat{\mathbf{d}}$, different constraints on \mathcal{H}_{eff} are implicitly imposed. We compare the behavior of five different settings, they are: 1.) $\mathcal{H}_{\text{random}}$, where \mathbf{d} is randomly sampled from $\mathcal{D}_{\text{pool}}$; 2.) $\mathcal{H}_{\text{hard}}$ where only hard examples can be sampled; 3.) $\mathcal{H}_{\text{easy}}$, opposite to the hard setting; 4.) $\mathcal{H}_{\text{easylong}}$, where the easy acronyms with longer lengths are more likely to be sampled; 5.) $\mathcal{H}_{\text{easyshort}}$, opposite to the easy-long setting.

See the first several columns of Table 2 that show the ratio of easy examples in \mathbf{d}^t . Compared with the random setting, all methods expect $\mathcal{H}_{\text{hard}}$ finally converges to \mathbf{d}^t with more easy examples, which means the bias towards easier acronyms would be amplified when \mathcal{H}_{eff} doesn’t impede it. On the contrary, using $\mathcal{H}_{\text{hard}}$ successfully restrain this bias, as the average number of easy samples in \mathbf{d}^t is even lower than that in \mathbf{d}^0 . We can also design composite \mathcal{H}_{eff} by choosing two properties of the data. For example, $\mathcal{H}_{\text{easylong}}$ restrains the samples with hard and short outputs, which is why they have more easy but long examples in their \mathbf{d}^t .

In summary, this experiment verifies that the Bayesian-IL framework still works when h is hidden: the bias is amplified generation by generation, implicitly imposing \mathcal{H}_{eff} can still guide the evolution direction. Please also refer to Appendix E for more results and discussions.

7. Conclusion

This paper examines the potential and ongoing evolutions of LLM agents by drawing parallels with human cultural evolution, where the latter is a well-established subject in cognitive science. By demonstrating that the sampling and learning procedures of LLMs in various algorithms can be

Table 2: Results when adding different \mathcal{H}_{eff} . We color the **highest** and **lowest** numbers in each column differently. Results under different settings are in Table 4 and 5.

$N_c =$	Ratio-easy					Avg-rank					Avg-length				
	2	4	6	8	10	2	4	6	8	10	2	4	6	8	10
Random	0.913±0.01	0.600±0.08	0.963±0.00	0.887±0.03	0.825±0.06	13519	27269	7487	10425	15871	5.425±1.04	4.825±0.33	5.600±1.55	5.014±1.50	4.713±0.63
Imitation-only	0.438±0.20	0.935±0.01	0.925±0.00	0.975±0.00	0.963±0.00	35235	7497	9081	5549	8075	4.450±0.86	4.175±0.13	4.188±0.65	5.438±1.24	4.387±1.40
Hard	0.219±0.19	0.250±0.43	0.450±0.43	0.338±0.16	0.500±0.23	49869	46436	37288	41255	31903	4.630±1.54	5.788±1.39	4.675±0.40	4.388±0.60	5.200±0.42
Easy	0.763±0.17	1.000±0.00	0.988±0.00	1.000±0.00	0.990±0.00	15910	3156	2383	2924	2650	3.925±0.33	5.263±0.06	4.713±0.06	4.240±0.08	4.893±0.71
Easy-long	0.988±0.00	0.975±0.00	0.988±0.00	0.988±0.00	1.000±0.00	7063	9413	8649	6898	7404	5.209±0.41	5.888±0.52	6.838±1.10	6.979±1.57	7.695±1.70
Easy-short	1.000±0.00	1.000±0.00	0.975±0.00	1.000±0.00	0.988±0.00	5671	4223	5733	4502	5251	3.975±0.50	4.012±1.03	4.374±0.50	3.950±0.03	4.250±0.24

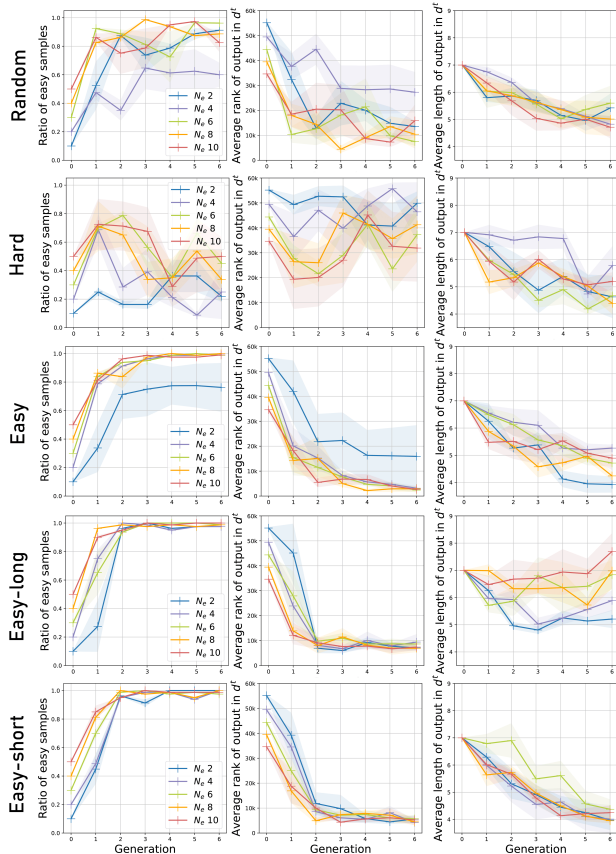


Figure 5: Results when adding different interaction phases of self-play among GPT3.5 agents. More results of self-play among Claude3 agents and interactions between GPT3.5 and Claude3 can be found in Figure 19.

effectively approximated by Bayesian inference, we successfully apply the Bayesian-IL framework to elucidate and steer the evolution of LLM agents. The presented theory and accompanying experiments not only provide deeper insights into LLM behavior from a top-down perspective but also hold the potential to inspire the design of more efficient self-evolution algorithms.

Impact Statement This paper presents work whose goal is to advance the field of machine learning. Although there are many potential societal consequences of large language models, and our work is potentially a step towards the possibility of steering them in desired directions (which could

potentially be positive or negative, depending on who steers them and the final efficacy of these approaches) our research is initial enough that we feel it is fruitless to make specific predictions at this point.

References

Beppu, A. and Griffiths, T. Iterated learning and the cultural ratchet. In *Proceedings of the Annual Meeting of the Cognitive Science Society*, volume 31, 2009.

Bonawitz, E., Denison, S., Griffiths, T. L., and Gopnik, A. Probabilistic models, learning algorithms, and response variability: sampling in cognitive development. *Trends in cognitive sciences*, 18(10):497–500, 2014.

Burns, C., Izmailov, P., Kirchner, J. H., Baker, B., Gao, L., Aschenbrenner, L., Chen, Y., Ecoffet, A., Joglekar, M., Leike, J., et al. Weak-to-strong generalization: Eliciting strong capabilities with weak supervision. *arXiv preprint arXiv:2312.09390*, 2023.

Carlsson, E., Dubhashi, D., and Regier, T. Iterated learning and communication jointly explain efficient color naming systems. *arXiv preprint arXiv:2305.10154*, 2023.

Chen, Z., Deng, Y., Yuan, H., Ji, K., and Gu, Q. Self-play fine-tuning converts weak language models to strong language models. *arXiv preprint arXiv:2401.01335*, 2024.

Chenhao, Z., Jieyu, Z., Aniruddha, K., and Ranjay, K. Iterated learning improves compositionality in large vision-language models. *arXiv preprint arXiv:2402.04792*, 2024.

Davies, M. The corpus of contemporary american english. 2008. URL www.english-corpora.org/coca/.

Dong, H., Xiong, W., Goyal, D., Pan, R., Diao, S., Zhang, J., Shum, K., and Zhang, T. Raft: Reward ranked fine-tuning for generative foundation model alignment. *arXiv preprint arXiv:2304.06767*, 2023.

Fay, N., Garrod, S., Roberts, L., and Swoboda, N. The interactive evolution of human communication systems. *Cognitive science*, 34(3):351–386, 2010.

Ferdinand, V., Kirby, S., and Smith, K. Regularization in language evolution: On the joint contribution of domain-specific biases and domain-general frequency learning.

- In *Evolution of Language: Proceedings of the 10th International Conference (EVOLANG10)*, pp. 435–436. World Scientific, 2014.
- Ferdinand, V., Kirby, S., and Smith, K. The cognitive roots of regularization in language. *Cognition*, 184:53–68, 2019.
- Gilks, W. R., Richardson, S., and Spiegelhalter, D. *Markov chain Monte Carlo in practice*. CRC press, 1995.
- Griffiths, T. L. and Kalish, M. L. Language evolution by iterated learning with bayesian agents. *Cognitive science*, 31(3):441–480, 2007.
- Griffiths, T. L., Christian, B. R., and Kalish, M. L. Using category structures to test iterated learning as a method for identifying inductive biases. *Cognitive Science*, 32(1): 68–107, 2008.
- Griffiths, T. L., Zhu, J.-Q., Grant, E., and McCoy, R. T. Bayes in the age of intelligent machines. *arXiv preprint arXiv:2311.10206*, 2023.
- Gulcehre, C., Paine, T. L., Srinivasan, S., Konyushkova, K., Weerts, L., Sharma, A., Siddhant, A., Ahern, A., Wang, M., Gu, C., et al. Reinforced self-training (rest) for language modeling. *arXiv preprint arXiv:2308.08998*, 2023.
- Guo, S., Ren, Y., Havrylov, S., Frank, S., Titov, I., and Smith, K. The emergence of compositional languages for numeric concepts through iterated learning in neural agents. *The 3rd workshop on Emergent Communication, NeurIPS*, 2019.
- Guo, S., Zhang, B., Liu, T., Liu, T., Khalman, M., Llinares, F., Rame, A., Mesnard, T., Zhao, Y., Piot, B., et al. Direct language model alignment from online ai feedback. *arXiv preprint arXiv:2402.04792*, 2024.
- Kirby, S., Dowman, M., and Griffiths, T. L. Innateness and culture in the evolution of language. *Proceedings of the National Academy of Sciences*, 104(12):5241–5245, 2007.
- Kirby, S., Cornish, H., and Smith, K. Cumulative cultural evolution in the laboratory: An experimental approach to the origins of structure in human language. *PNAS*, 105 (31):10681–10686, 2008.
- Kirby, S., Tamariz, M., Cornish, H., and Smith, K. Compression and communication in the cultural evolution of linguistic structure. *Cognition*, 141:87–102, 2015.
- Lewis, D. *Convention: A philosophical study*. John Wiley & Sons, 2008.
- Lu, Y., Singhal, S., Strub, F., Courville, A., and Pietquin, O. Countering language drift with seeded iterated learning. In *International Conference on Machine Learning*, pp. 6437–6447. PMLR, 2020.
- Madaan, A., Tandon, N., Gupta, P., Hallinan, S., Gao, L., Wiegrefe, S., Alon, U., Dziri, N., Prabhunoye, S., Yang, Y., et al. Self-refine: Iterative refinement with self-feedback. *arXiv preprint arXiv:2303.17651*, 2023.
- McCoy, R. T., Yao, S., Friedman, D., Hardy, M., and Griffiths, T. L. Embers of autoregression: Understanding large language models through the problem they are trained to solve. *arXiv preprint arXiv:2309.13638*, 2023.
- Mobahi, H., Farajtabar, M., and Bartlett, P. Self-distillation amplifies regularization in hilbert space. *Advances in Neural Information Processing Systems*, 33:3351–3361, 2020.
- Motamedi, Y., Schouwstra, M., Smith, K., Culbertson, J., and Kirby, S. Evolving artificial sign languages in the lab: From improvised gesture to systematic sign. *Cognition*, 192:103964, 2019.
- Motamedi, Y., Wolters, L., Naegeli, D., Kirby, S., and Schouwstra, M. From improvisation to learning: How naturalness and systematicity shape language evolution. *Cognition*, 228:105206, 2022.
- Navarro, D. J., Perfors, A., Kary, A., Brown, S. D., and Donkin, C. When extremists win: Cultural transmission via iterated learning when populations are heterogeneous. *Cognitive Science*, 42(7):2108–2149, 2018.
- Nielsen, S. F. The stochastic em algorithm: estimation and asymptotic results. *Bernoulli*, pp. 457–489, 2000.
- Park, J. S., O’Brien, J., Cai, C. J., Morris, M. R., Liang, P., and Bernstein, M. S. Generative agents: Interactive simulacra of human behavior. In *Proceedings of the 36th Annual ACM Symposium on User Interface Software and Technology*, pp. 1–22, 2023.
- Perfors, A., Tenenbaum, J. B., Griffiths, T. L., and Xu, F. A tutorial introduction to bayesian models of cognitive development. *Cognition*, 120(3):302–321, 2011.
- Qiu, L., Jiang, L., Lu, X., Sclar, M., Pyatkin, V., Bhagavatula, C., Wang, B., Kim, Y., Choi, Y., Dziri, N., et al. Phenomenal yet puzzling: Testing inductive reasoning capabilities of language models with hypothesis refinement. *International Conference on Learning Representations*, 2024.
- Reali, F. and Griffiths, T. L. The evolution of frequency distributions: Relating regularization to inductive biases through iterated learning. *Cognition*, 111(3):317–328, 2009.

- Ren, Y., Guo, S., Labeau, M., Cohen, S. B., and Kirby, S. Compositional languages emerge in a neural iterated learning model. In *International Conference on Learning Representations*, 2020.
- Ren, Y., Lavoie, S., Galkin, M., Sutherland, D. J., and Courville, A. Improving systematic generalization using iterated learning and simplicial embeddings. In *Thirty-seventh Conference on Neural Information Processing Systems*, 2023.
- Shumailov, I., Shumaylov, Z., Zhao, Y., Gal, Y., Papernot, N., and Anderson, R. Model dementia: Generated data makes models forget. *arXiv preprint arXiv:2305.17493*, 2023.
- Touvron, H., Martin, L., Stone, K., Albert, P., Almahairi, A., Babaei, Y., Bashlykov, N., Batra, S., Bhargava, P., Bhosale, S., et al. Llama 2: Open foundation and fine-tuned chat models. *arXiv preprint arXiv:2307.09288*, 2023.
- Van der Vaart, A. W. *Asymptotic statistics*, volume 3. Cambridge university press, 2000.
- Vani, A., Schwarzer, M., Lu, Y., Dhekane, E., and Courville, A. Iterated learning for emergent systematicity in vqa. *International Conference on Learning Representations*, 2021.
- Wang, Y., Kordi, Y., Mishra, S., Liu, A., Smith, N. A., Khashabi, D., and Hajishirzi, H. Self-instruct: Aligning language model with self generated instructions. *arXiv preprint arXiv:2212.10560*, 2022.
- Weizhe, Y., Richard, Yuanzhe, P., Kyunghyun, C., Sainbayar, S., Jing, X., and Jason, W. Self-rewarding language models. In *arXiv preprint arXiv:2401.10020*, 2024.
- Xie, S. M., Raghunathan, A., Liang, P., and Ma, T. An explanation of in-context learning as implicit bayesian inference. In *International Conference on Learning Representations*, 2022.
- Xiong, W., Dong, H., Ye, C., Zhong, H., Jiang, N., and Zhang, T. Gibbs sampling from human feedback: A provable kl-constrained framework for rlhf. *arXiv preprint arXiv:2312.11456*, 2023.
- Xu, C., Guo, D., Duan, N., and McAuley, J. Baize: An open-source chat model with parameter-efficient tuning on self-chat data. *arXiv preprint arXiv:2304.01196*, 2023.
- Xu, W., Zhu, G., Zhao, X., Pan, L., Li, L., and Wang, W. Y. Perils of self-feedback: Self-bias amplifies in large language models. *arXiv preprint arXiv:2402.11436*, 2024.
- Zhang, C., Jia, B., Edmonds, M., Zhu, S.-C., and Zhu, Y. Acre: Abstract causal reasoning beyond covariation. In *Proceedings of the IEEE/CVF Conference on Computer Vision and Pattern Recognition*, pp. 10643–10653, 2021.

A. Common concerns of the proposed theory and its applicability to real methods

A.1. Assumptions of Bayesian-IL and practical scenarios

As typical in theoretical machine learning research, some assumptions are needed to prove results about models’ behavior; these assumptions are often not *exactly* satisfied by practical algorithms. So, we elaborate here on the important assumptions we made and when practical algorithms break them.

1. Assumptions for the theory. To derive the guarantees of Proposition 1, we first model the interaction phase as a binary filter on $h \in \mathcal{H}_{\text{eff}}$ and also assume a shared prior $P_0(h)$ among all agents involved in Bayesian-IL. We also model the LLM’s in-context behavior as a Bayesian agent and assume the number of samples during the imitation phase is sufficient.

2. Assumptions we can break for iterative ICL experiments.

- Binary filter on $h \in \mathcal{H}_{\text{eff}}$. All our LLM experiments break this assumption (the pure Bayesian example in Appendix C.2 does not). For example, in the ACRE experiments, we use self-refine and hypothesis search as the interaction phase. Self-refine asks the model to evaluate the responses, and the hypothesis search uses an external interpreter: they both manipulate h by feeding messages to the LLM, rather than a binary filter. (When using an external interpreter, h is usually filtered before forming the refinement feedback.) For the experiments in Section 6, where the h is implicit, we re-rank all the generated samples in $\mathcal{D}_{\text{pool}}$ and take a weighted sample during imitation, similar to re-ranking the generated examples in ReST. Since all these interaction designs are commonly applied in the community, and our theory describes their qualitative behaviors well despite strictly violating the assumption, we believe our methods can shed more light on other practical methods with similar designs.
- Identical $P_0(h)$ for agents in different generations. Although this assumption makes it easier to derive Proposition 1, slightly relaxing it will not change the whole story: we only require different agents to share a similar tendency towards a specific bias. To verify this, we conduct several experiments when the agents in different generations are different LLMs (e.g., GPT3.5 plays with Claude3 in Appendix D and E). The phenomena claimed by the theory still hold.

3. Assumptions we can break in the future. The assumption that LLM learns in a Bayesian way when conducting ICL is important for our current analysis. The parallel between iterated learning and the EM algorithm relies on this assumption. However, our analysis could be extended to iterated in-weights learning (iIWL for short). Note that many related works already mentioned the observations of increased bias or decreased creativity during iterated finetuning (Touvron et al., 2023). From the theory perspective, although there are many finetuning methods, e.g., SFT, RLHF, DPO, etc., their aims are consistent: increasing the likelihood of $p(\mathbf{d}_{\text{train}} | h)$ under instructions. However, as these methods have different loss functions, their learning dynamics might also be distinct. We left the exploration of them in our future work.

A.2. Why the tasks in this paper look so "toyish"

The main reason is that we want to directly observe some quantitative numbers described by the theory. For the explicit h case, we chose the ACRE task because of its simple \mathcal{H} , making it possible to observe the distribution and entropy of all possible h . We believe observing the model’s logits supports our theory more directly than merely observing the accuracy or other quantitative metrics.

For the implicit h case, we chose the acronym task, which is a prototype of self-data-augmentation in self-instruct. We initially consider the conditional creative writing task (quite common in many related works), where the model needs to write a passage (i.e., the list in our settings) based on several topic words (i.e., the acronym). However, constrained by the context length of LLMs, we can’t generate more than 4 examples in one generation, which makes it hard to calculate the statistics of \mathbf{d}^t . Remember the model will generate 20 extra \mathbf{d}^t based on 20 \mathbf{d}^{t-1} in our acronym experiments. In summary, although the experiments studied in our paper look artificial, they are reasonable approximations of real tasks.

Last, in a concurrent work Xu et al. (2024), the authors study practical applications like machine translation, creative writing, math reasoning, etc, in an iterative ICL setting. Their observations match our theoretical analysis quite well: bias is amplified generation by generation, and introducing external feedback can mitigate it. However, due to the complexity of the tasks they considered, they can only observe the average bias and the skew level using several conclusive quantitative metrics. Hence we believe that by combining our theoretical analysis, detailed observations on artificial examples, and the evidence from real applications in Xu et al. (2024), one can draw a good overview of how LLM would evolve in an iterated ICL setting.

A.3. How our analysis brings benefits to practical algorithms

Although not strictly proven to be effective, our experiments and analysis provide the following potential approaches to guide the model’s evolution:

- Select \mathbf{d}^0 that makes more *confident and correct* predictions on the target task. Manually selecting good in-context examples is intuitive. Our analysis, though, suggests taking the model’s confidence (i.e., the logits) into account, because the theory claims that the likelihood and bias in prior are competing with each other during evolution. From Figure 3, we see the model evolves faster if the likelihood of $\mathbf{d}^0 \mid h^*$ is weaker. The results in Figure 4 also provide similar insights: the related biases are amplified slower when the number of easy samples in \mathbf{d}^0 decreases.
- Designing a good interaction phase is important: more accurate \mathcal{H}_{eff} leads to better performance. This can be supported by comparing self-refine and hypothesis-search in our paper. The paper Xu et al. (2024) also claims that external feedback with more accurate assessments or feedback from a larger model can reduce the amplified bias.
- Manipulating the instruction prompt: in our analysis, both $P_0(h)$ and $P_{l_m}(h)$ are the model’s predictions conditioned on the instruction prompt \mathbf{w} . Hence adding preference in the task instruction (or changing the system prompt) during evolution could be an effective way of guiding the model’s evolution. Our ACRE experiments show the feasibility of this: remember we can introduce spurious correlation by adding one sentence to the instruction. Hence it is also possible to guide the model’s evolution by feeding appropriate prompts during learning and sampling. Plus, authors of Guo et al. (2024) also showed in Figure 6 that adding the bias by manipulating the instruction prompt can guide the model to provide more short and helpful responses, which counters the model’s inborn bias towards long responses.
- Manipulating the temperature: Bayesian-IL theory studies the evolution of the distribution, so the temperature should also be an important factor for the evolution, as illustrated in Figure 2. We left the exploration between temperature and different phases in IL in the future.

B. Proofs related to Bayesian Agents

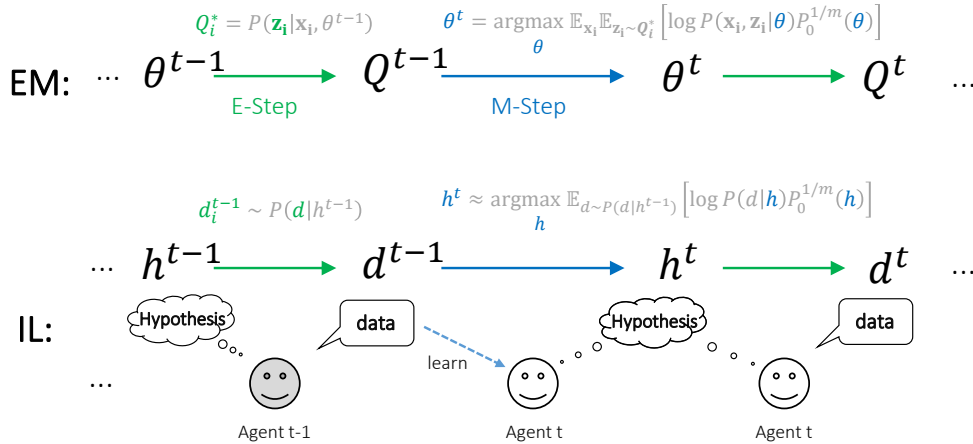


Figure 6: Illustrations of typical EM algorithm and an imitation-only iterated learning method.

B.1. Recap the Proof of Expectation-Maximization Algorithm

To get a clear picture of the asymptotic behavior of imitation-only iterated learning, we first recap how a typical expectation-maximization (EM) algorithm converges when the target function is posterior distribution⁶. Consider a statistical model that generates a set of observable data samples $\{\mathbf{x}_i\}_{i=1}^m$ and the corresponding hidden variables $\{\mathbf{z}_i\}_{i=1}^m$. The generating mechanism can be expressed as $P(\mathbf{x} | \mathbf{z}, \theta)$, where θ is a set of unknown parameters determining this distribution. To get a

⁶The MLE (maximum likelihood estimation) version of the EM algorithm is more common in textbooks.

MAP(maximum a posterior) estimation of θ , we need to optimize the following target function:

$$\begin{aligned}
 \mathcal{L}(\theta) &= \log P(\theta \mid \mathbf{x}_1, \dots, \mathbf{x}_m) \\
 &= \log P_0(\theta) + \log P(\mathbf{x}_1, \dots, \mathbf{x}_m \mid \theta) - \log P(\mathbf{x}_1, \dots, \mathbf{x}_m) \\
 &= \sum_{i=1}^m \frac{1}{m} \log P_0(\theta) + \sum_{i=1}^m \log P(\mathbf{x}_i \mid \theta) - \log P(\mathbf{x}_1, \dots, \mathbf{x}_m) \\
 &= \sum_{i=1}^m \log \left(P(\mathbf{x}_i \mid \theta) P_0^{\frac{1}{m}}(\theta) \right) - \log P(\mathbf{x}_1, \dots, \mathbf{x}_m)
 \end{aligned} \tag{4}$$

where $P_0(\theta)$ is the prior distribution of parameters. As the marginal distribution $P(\mathbf{x}_i \mid \theta)$ is hard to calculate due to the existence of the hidden variable \mathbf{z}_i , our target function can then be expressed as

$$\tilde{\mathcal{L}}(\theta) = \mathcal{L}(\theta) + \text{const} = \sum_{i=1}^m \log \left(\sum_{\mathbf{z}_i} P(\mathbf{x}_i, \mathbf{z}_i \mid \theta) P_0^{\frac{1}{m}}(\theta) \right) \tag{5}$$

where the term $\log P(\mathbf{x}_1, \dots, \mathbf{x}_m)$ is eliminated as it doesn't depend on θ . The target function above is still hard to tackle due to the summation inside the logarithmic function. To solve this, we first introduce an auxiliary function $Q_i(\mathbf{z}_i)$, which is a probability distribution over \mathbf{z}_i , and reformulate the target as

$$\tilde{\mathcal{L}}(\theta) = \sum_{i=1}^m \log \left(\sum_{\mathbf{z}_i} Q_i(\mathbf{z}_i) \frac{P(\mathbf{x}_i, \mathbf{z}_i \mid \theta) P_0^{\frac{1}{m}}(\theta)}{Q_i(\mathbf{z}_i)} \right) = \sum_{i=1}^m \log \left(\mathbb{E}_{\mathbf{z}_i \sim Q_i} \left[\frac{P(\mathbf{x}_i, \mathbf{z}_i \mid \theta) P_0^{\frac{1}{m}}(\theta)}{Q_i(\mathbf{z}_i)} \right] \right). \tag{6}$$

Given the concavity of the logarithmic function, we can use Jensen's inequality to get a lower bound of $\tilde{\mathcal{L}}(\theta)$:

$$\tilde{\mathcal{L}}(\theta) \geq \mathcal{J}(\theta, Q) = \sum_{i=1}^m \mathbb{E}_{\mathbf{z}_i \sim Q_i} \left[\log \frac{P(\mathbf{x}_i, \mathbf{z}_i \mid \theta) P_0^{\frac{1}{m}}(\theta)}{Q_i(\mathbf{z}_i)} \right]. \tag{7}$$

The EM algorithm then maximizes this lower bound by alternatively optimizing θ and Q_i for several rounds.

In the **E-step**, as illustrated in Figure 6, we use the estimated θ^{t-1} in the previous round to find $Q_i^* = \operatorname{argmax}_Q \mathcal{J}(\theta^{t-1}, Q)$. Specifically, we need to push this lower bound to be tight by making the equality in Equation (7) hold. Following the properties of Jensen's inequality, the equality only holds when $\frac{P(\mathbf{x}_i, \mathbf{z}_i \mid \theta^{t-1}) P_0^{\frac{1}{m}}(\theta)}{Q_i(\mathbf{z}_i)}$ is a constant. Combining this requirement and the fact that $\sum_{\mathbf{z}_i} Q_i(\mathbf{z}_i) = 1$, we can calculate the optimal $Q_i^*(\mathbf{z}_i) = P(\mathbf{z}_i \mid \mathbf{x}_i, \theta^{t-1})$, which is the posterior distribution of \mathbf{z}_i given the observable data \mathbf{x}_i and the fixed parameters θ^{t-1} .

In the **M-step**, we plug in the estimated Q_i^* to $\mathcal{J}(\theta, Q)$ to get the target function as:

$$\mathcal{J}(\theta; Q^*) = \sum_{i=1}^m \mathbb{E}_{\mathbf{z}_i \sim Q_i^*} \left[\log \frac{P(\mathbf{x}_i, \mathbf{z}_i \mid \theta) P_0^{\frac{1}{m}}(\theta)}{Q_i^*} \right] = \sum_{i=1}^m \mathbb{E}_{\mathbf{z}_i \sim Q_i^*} \left[\log \left(P(\mathbf{x}_i, \mathbf{z}_i \mid \theta) P_0^{\frac{1}{m}}(\theta) \right) \right] - c, \tag{8}$$

where $c = \mathbb{E}_{\mathbf{z}_i \sim Q_i^*} [Q_i^*]$ is a constant term and can be neglected while optimizing θ . In this step, we can calculate $\theta^t = \operatorname{argmax}_\theta \mathcal{J}(\theta; Q^*)$ using gradient descent or other parameter estimation methods.

In summary, the E-step ensures a tight lower bound $\mathcal{J}(\theta, Q)$ and the M-step finds better θ to make it larger. The two steps cooperate to ensure a series of estimations of θ for which $\mathcal{L}(\theta)$ is non-decreasing. Finally, the estimation of parameters will converge to the one that maximizes the posterior distribution, i.e., $\mathbb{E}(\theta^*) = \operatorname{argmax}_\theta P(\theta \mid \mathbf{x}_1, \dots, \mathbf{x}_m)$, if it is convex.

B.2. Proof: Convergence Behavior of Bayesian Agents in Iterated Learning

Proposition 1. Consider several Bayesian agents sharing the same prior $P_0(h)$ are conducting iterated learning for T generations. If T is sufficiently large, then no matter the choice of \mathbf{d}^0 , any agent t with $t > T$ will have

$$P_{lm}(h) \rightarrow \mathbf{1}(h = h^{T*})$$

where h^{T*} is a stationary point (e.g. a local maximum) of $P_0(h)$ subject to $h \in \mathcal{H}_{\text{eff}}$.

Proof. The proof of this proposition can be divided into two steps. In the first step, we show that imitation-only iterated learning shares similar convergence behavior with a standard EM algorithm. In the second step, we show the “selecting” pressure introduced via the interaction phase doesn’t break the necessary conditions of the convergence in the first step. Merging these two steps leads to the proposition.

Step 1: imitation-only iterated learning as a special EM

Recall the imitation-only iterated learning illustrated in the bottom part in Figure 6, where the hypothesis held by the agent in the $(t - 1)$ -th generation is represented by h^{t-1} . With this hypothesis, the agent will generate m data samples using $P(d | h^{t-1})$, denoted $\mathbf{d}^{t-1} \triangleq [d_1^{t-1}, \dots, d_m^{t-1}]$. In the t -th generation, a new agent will first update its posterior probability using $P(h | \mathbf{d}^{t-1})$, and then select h^t by picking the one with the largest posterior. As there are multiple data samples in \mathbf{d}^{t-1} , this process can be expressed as

$$\begin{aligned}
 h^t &= \operatorname{argmax}_h \log P(h | d_1^{t-1}, d_2^{t-1}, \dots, d_m^{t-1}) & (9) \\
 &= \operatorname{argmax}_h \log \left(\frac{p(d_1^{t-1}, d_2^{t-1}, \dots, d_m^{t-1} | h) P_0(h)}{P(d_1^{t-1}, d_2^{t-1}, \dots, d_m^{t-1})} \right) \\
 &= \operatorname{argmax}_h \log \left(P_0(h) \prod_{i=1}^m p(d_i^{t-1} | h) \right) \\
 &= \operatorname{argmax}_h \frac{1}{m} \log P_0(h) + \frac{1}{m} \sum_{i=1}^m \log p(d_i^{t-1} | h) \\
 &\approx \operatorname{argmax}_h \mathbb{E}_{d \sim p(d|h^{t-1})} [\log P_0^{\frac{1}{m}}(h)] + \mathbb{E}_{d \sim p(d|h^{t-1})} [\log p(d | h)] \\
 &= \operatorname{argmax}_h \mathbb{E}_{d \sim p(d|h^{t-1})} [\log p(d | h) P_0^{\frac{1}{m}}(h)]. & (10)
 \end{aligned}$$

Based on the analysis above, we notice that the imitation-only iterated learning and the EM algorithm are almost identical: by replacing θ and \mathbf{z} to h and \mathbf{d} , and by removing the random variable \mathbf{x} ⁷, we can also have similar theoretical guarantees for the imitation-only iterated learning algorithm.

To prove this, we can first verify the equivalence between the imitation phase and an M-step. By comparing the target functions when calculating hidden variables (h and θ) in these two algorithms, i.e., Equation (8) and (10), we can find two major differences. First, the expectation of observable samples (i.e., $\mathbb{E}_{\mathbf{x}_i}$) disappears in Equation (10), as we assume there are no “observations” in iterated learning. We can also introduce a dummy variable named \mathbf{x} to the iterated learning process, and find that the existence of \mathbf{x} doesn’t influence the aforementioned calculation at all. Second, in IL, we can only approximate $\mathbb{E}_{d_i^{t-1}}[\cdot]$ by sampling d from $p(d | h^{t-1})$, while in EM, the posterior distribution $P(\mathbf{z}_i | \mathbf{x}_i, \theta^t)$ is usually analytically calculated. Of this discrepancy, if our \mathbf{d} is a good approximation of $p(d | h^{t-1})$, the imitation phase in IL is equivalent to an M-step in EM.

We then verify whether the transmission phase is a good approximation of an E-step. The first thing to check is the tightness of the lower bound generated via Jensen’s inequality, which guarantees the non-decreasing update of the target function across multiple generations. we can first assume the target function of the whole iterated learning process is

⁷It is unusual to apply EM with no observable data, but removing it doesn’t violate any assumptions in the derivation of EM.

$\mathcal{L}(h) = \log P_0(h)$, and derives its lower bound $\mathcal{J}(h; Q)$ following a similar procedure in EM:

$$\begin{aligned}
 \mathcal{L}(h) &= \log P_0(h) \\
 &= m \log P_0^{\frac{1}{m}}(h) \\
 &= m \log \left(\sum_{d_i} p(d_i | h) P_0^{\frac{1}{m}}(h) \right) \\
 &= m \log \left(\sum_{d_i} Q_i(d_i) \frac{p(d_i | h) P_0^{\frac{1}{m}}(h)}{Q_i(d_i)} \right) \\
 &= m \log \mathbb{E}_{d_i \sim Q_i} \left[\frac{p(d_i | h) P_0^{\frac{1}{m}}(h)}{Q_i(d_i)} \right] \\
 &\geq \mathbb{E}_{d_i \sim Q_i} \log \left[\frac{p(d_i | h) P_0^{\frac{1}{m}}(h)}{Q_i(d_i)} \right] \triangleq \mathcal{J}(h, Q)
 \end{aligned} \tag{11}$$

The equality of Jensen’s inequality holds when $\frac{p(d_i|h)P_0^{1/m}(h)}{Q_i(d_i)}$ is a constant. Using the fact that $\sum_{d_i} Q_i(d_i) = 1$, we can have the optimal $Q_i^* = p(d_i | h)$. In summary, as we sample each $d_i^{t-1} \sim p(d | h^{t-1})$, the transmission phase in IL is equivalent to an E-step in EM.

Another interesting parameter to discuss is m , i.e., the number of data samples generated by an agent in each generation. The choice of m determines how well the sampled \mathbf{d} can represent the ground truth $p(d | h)$. For large enough m , we can prove the convergence guarantee using the above procedure. When $m = 1$, the standard EM algorithm becomes a stochastic EM approximation (Gilks et al., 1995). The authors of Nielsen (2000) proved that in stochastic EM, θ in different generations form a homogeneous Markov chain whose stationary distribution over hypotheses is approximately centered on the maximum-likelihood solution. In other words, when $t > T$ for sufficiently large T , $\mathbb{E}[\theta^t]$ optimizes $\mathbb{E}_{\mathbf{x}}[P(\theta | \mathbf{x}_1, \dots, \mathbf{x}_m)]$, and similarly, $\mathbb{E}[h^t]$ is the optimizer of $P_0(h)$. In other words, the dominating hypothesis in imitation-only iterated learning converges to the one with the highest prior, which is equivalent to the large m case.

Although $m = 1$ doesn’t influence the converged estimation of h , a too small m will make the variance of estimation large, and hence impede the converging speed of h . Then should we choose m as large as possible? The answer is still no: too large m will also impede the converging speed. We can get some intuition by observing Equation (10), where $P_0^{1/m}(h)$ determines the effect of the prior when selecting optimal h in each generation. If m is too large, this distribution would be very flat and the preference encoded in the prior cannot influence the choice of h in this generation much – the likelihood term $P(d | h)$ will dominate.⁸ Hence the resulting h^t would be quite close to h^{t-1} , which means the evolution of belief on h would be slow.

Actually, the choice of m is usually considered as the “bottleneck” parameter in different iterated learning algorithms. Almost all the related studies point out that the bottleneck should not be too wide or too tight (like experiments in Kirby et al. (2015) and Ren et al. (2020)). Our Bayesian analysis provides a theoretical explanation of the effect.

Step 2: the influence of introducing \mathcal{H}_{eff} . Let us first check the imitation phase, i.e., the E-step where h^t is calculated in Equation (9). Assume we have a perfect interaction phase that can rule out all $h \notin \mathcal{H}_{\text{eff}}$, then the target function is:

⁸A similar trend also exists in Bernstein-von Mises theorem (see e.g. Van der Vaart, 2000), which claims the posterior $p(\theta | x_1, \dots, x_n) = \mathcal{N}(\theta_0, n^{-1}I(\theta_0)^{-1})$, for $n \rightarrow \infty$. In other words, $P(h|d_1, \dots, d_m)$ would become peakier as m increases, and hence h^t will be closer to h^{t-1} after the imitation phase.

$$\begin{aligned}
 h^t &= \operatorname{argmax}_{h \in \mathcal{H}_{\text{eff}}} \log P(h \mid d_1^{t-1}, d_2^{t-1}, \dots, d_m^{t-1}) \\
 &= \operatorname{argmax}_h \log P(h \mid d_1^{t-1}, d_2^{t-1}, \dots, d_m^{t-1}) \cdot \mathbb{1}(h \in \mathcal{H}_{\text{eff}}) \\
 &= \operatorname{argmax}_h \mathbb{E}_{d \sim p(d|h^{t-1})} \left[\log p(d \mid h) \cdot \left(P_0^{\frac{1}{m}}(h) \cdot \mathbb{1}(h \in \mathcal{H}_{\text{eff}}) \right) \right] \\
 &\triangleq \operatorname{argmax}_h \mathbb{E}_{d \sim p(d|h^{t-1})} \left[\log p(d \mid h) \cdot \tilde{P}_0^{\frac{1}{m}}(h) \right],
 \end{aligned} \tag{12}$$

where we define a ‘‘regularized’’ prior as $\tilde{P}_0(h) \triangleq c \cdot P_0(h) \cdot \mathbb{1}(h \in \mathcal{H}_{\text{eff}})$. Then, by substituting this prior back to $\mathcal{L}(h)$ defined in Equation (11), we find the optimal $Q_i^* = p(d_i \mid h)$ still holds. In other words, as long as we same $d_i^{t-1} \sim p(d \mid h^{t-1})$, where $h^{t-1} \in \mathcal{H}_{\text{eff}}$, all the conditions required for this proposition still hold. Furthermore, this proof also provides us an insight that adding constraints on $h \in \mathcal{H}_{\text{eff}}$ is required in both imitation and transmission phases. Hence having a powerful ‘‘data-filter’’ or ‘‘data-ranking’’ design for the transmission phase would also make the evolution more robust, like those applied in RAFT (Dong et al., 2023) and ReST (Gulcehre et al., 2023). \square

B.3. Proof: LLM as a Bayesian Agent

Proposition 2. *Consider that agent A is conducting in-context learning. If the prompt examples in \mathbf{d}^{t-1} are generated by another agent B with the same prior knowledge (e.g., they come from the same checkpoint and use the same prompt), sampling from the posterior predictive distribution of agent A, i.e., $d^t \sim P_{lmw}(d \mid \mathbf{d}^{t-1})$, can be decomposed into: 1.) $h^{t*} \rightarrow \operatorname{argmax}_h P_{lmw}(h \mid \mathbf{d}^{t-1})$, and 2.) $d^t \sim P_{lmw}(d \mid h^{t*})$, where h is a hidden variable that describes the mapping between x and y .*

Proof. The proof of this proposition can be divided into two steps. In the first part, we de-marginalize the posterior predictive distribution on a hidden variable h , and then show that the model automatically ‘‘selects’’ a hypothesis h^{t*} that generates the prompting examples. In the second part, we show that when the examples in \mathbf{d}^{t-1} are generated by another LLM with the same prior belief over h , the MAP (maximize a posterior) estimation of h can approximate h^{t*} well.

Step 1: In our paper, we assume the query and answer sequences in each example, i.e., $d_i = (x_i, y_i)$, are controlled by the hidden hypothesis h , which plays a similar role to the ‘‘concept’’ parameter θ mentioned in Xie et al. (2022)⁹. Then the posterior predictive distribution can be decomposed as:

$$\begin{aligned}
 P(d \mid \mathbf{d}^{t-1}) &= \int_h p(d \mid \mathbf{d}^{t-1}, h) P(h \mid \mathbf{d}^{t-1}) dh \\
 &= \int_h p(d \mid h) P(h \mid \mathbf{d}^{t-1}) dh \\
 &\propto \int_h p(d \mid h) p(\mathbf{d}^{t-1} \mid h) P_0(h) dh \\
 &\propto \int_h p(d \mid h) \frac{p(\mathbf{d}^{t-1} \mid h)}{p(\mathbf{d}^{t-1} \mid h^{t*})} P_0(h) dh \\
 &= \int_h p(d \mid h) \exp(n \cdot r_n(h)) P_0(h) dh,
 \end{aligned} \tag{13}$$

where $r_n(h) \triangleq \frac{1}{n} \log \frac{p(\mathbf{d}^{t-1} \mid h)}{p(\mathbf{d}^{t-1} \mid h^{t*})}$. In Equation (13), the second line follows the Markov property of hypothesis and data samples, the third line follows the Bayesian rule and drops a constant term, the fourth line is generated by dividing a constant $p(\mathbf{d}^{t-1} \mid h^{t*})$, where h^{t*} is a hypothesis that generates \mathbf{d}^{t-1} . Now we see the $r_n(h)$ has almost the same form as $r_n(\theta)$ in Xie et al. (2022). By reusing the derivation in that paper (mainly in Section 3.2 and the proof of its Theorem 1), we can conclude that $\exp(n \cdot r_n(h)) \rightarrow 0$ for any $h \neq h^{t*}$ and $\exp(n \cdot r_n(h^{t*})) \rightarrow 1$. Hence Equation (13) becomes:

$$P(d \mid \mathbf{d}^{t-1}) = P(d \mid h^{t*}). \tag{14}$$

⁹As we only need the ‘‘selection’’ mechanism mentioned in this paper, the HMM (Hidden Markov Model) assumption is not required in our setting.

Step 2: In a general in-context learning setting, the prompting examples \mathbf{d}^{t-1} are usually sampled from an unknown distribution P_{prompt} . For example, by analyzing different x_{test} , the researchers can manually design effective prompting examples sharing similar chain-of-thought structures with the target question. Obviously, such P_{prompt} is impossible to parameterize or analyze accurately. To approximate it, Xie et al. (2022) first assumes that both the prompting examples and the pre-training corpus are natural languages, and a well-trained LLM can approximate this “natural language distribution” well. Then, P_{prompt} can be well approximated by $P(\cdot | \theta^*)$ under some θ^* , which is the prompt concept in that paper.

In our settings, as we assume the prompting examples \mathbf{d}^{t-1} are generated by another agent-B sharing the *same prior*, then the h^{t*} triggered by feeding \mathbf{d}^{t-1} to agent-A would be exactly the same as that feeding that to agent-B, i.e.,

$$h^{t*} = \underset{h}{\operatorname{argmax}} P_{lmw}(h | \mathbf{d}^{t-1}), \tag{15}$$

where P_{lmw} is model’s belief after receiving the common instruction \mathbf{w} .

Combining these two steps, we can decompose the sampling procedure $d^t \sim P(d | \mathbf{d}^{t-1})$ into two parts: first, inherently select h^{t*} based on observations generated by another agent in the previous generation; then sample new d conditioned on this h^{t*} , which matches the Bayesian-IL procedure discussed in this paper. \square

C. Experiments of Iterated Learning on Different Domains

To provide a panorama of iterated learning and its applications in different fields, this appendix will first give an intuitive explanation using some lab experimental results. Then, experiments on the emergence of compositional language among Bayesian agents are introduced to verify all the theoretical hypotheses.

C.1. Iterated Learning in Lab Experiments using Lewis Language Game

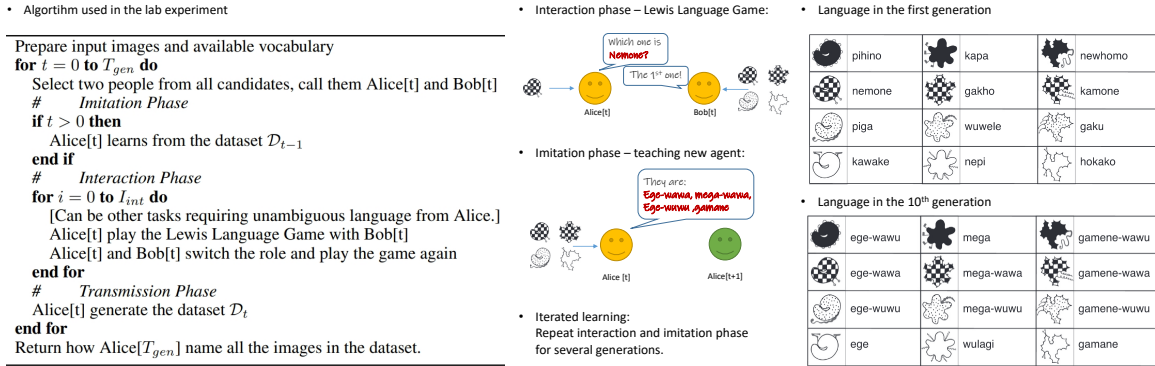


Figure 7: The lab experiments (algorithm, settings, and results) conducted in (Kirby et al., 2015).

As denoted in (Kirby et al., 2008), iterated learning is a process where one individual learns by observing the output of another individual, who learned in the same way. In this multiple-generation learning procedure, the shared language (i.e., h) among learning agents will gradually become more systematic under the compressibility pressure (imposed during imitation, embodied in $P_0(h)$) and expressivity pressure (imposed during interaction, requiring $h \in \mathcal{H}_{\text{eff}}$). To simulate this process, authors of (Kirby et al., 2015) design a two-phases learning procedure illustrated in Figure 7. In the interaction phase, the speaker (Alice) and listener (Bob) must cooperate to accomplish a Lewis referential game (see the middle panel in Figure 7). Specifically, Alice will first create a name for the given objects and talk that to Bob. After receiving this message, Bob needs to select the correct object shown to Alice among some candidates. If correct, both of them are rewarded. This phase terminates when they can achieve a high enough success rate. To succeed in this game, the shared language should be expressive enough to avoid any ambiguities – we expect the language to be a bijection. Then, we select another new naive candidate (Alice[t+1]) and let it learn the naming system created by Alice[t] and Bob[t]. In this phase, those highly structural mappings should be easier for a human to remember, which is how the compressibility pressure is imposed. After that, Alice[t+1] will play the same game with another Bob[t+1] and the interaction phase starts again. We provide the languages

generated by Alice[0] and Alice[10] in the right panel in Figure 7: it is clear that an interesting structure emerges in the language generated by Alice[10]. There are also plenty of similar lab experiments that support the “two pressures” and cultural evolution hypothesis using IL-like training methods, e.g., (Fay et al., 2010; Ferdinand et al., 2019; Motamedi et al., 2019; 2022). Although these methods have different types of input, game designs, learning procedures, vocabularies (like gesture language), etc., the conclusion of them is quite consistent: compressibility and expressivity pressures are crucial for the emergence of systematic mappings, iteratively learning and interacting can amplify these pressures a lot, which matches the Bayesian explanations well.

C.2. Iterated Learning of Bayesian Agents (re-implementation of results in Kirby et al. (2015))

To verify that the emergence of systematic mappings in iterated learning is not an accident, authors of (Beppu & Griffiths, 2009) provide a guarantee by analyzing the behavior of Bayesian agents. There are also plenty of related works in cognitive science, like (Bonawitz et al., 2014; Ferdinand et al., 2014; Navarro et al., 2018; Perfors et al., 2011; Realí & Griffiths, 2009), discussing the influence of and theories behind iterated learning and Bayesian analysis.

To give the readers a better understanding of how iterated learning works, we re-implement the Bayesian experiments mentioned in (Kirby et al., 2015). Consider the following toy example, where we have four different input objects: $\mathcal{X} = \{\text{blue circle, blue box, red circle, red box}\}$, and four possible names: $\mathcal{Y} = \{00, 01, 10, 11\}$. The hypothesis h is defined as $h \in \mathcal{H} : \mathcal{X} \rightarrow \mathcal{Y}$. In this example, we have $|\mathcal{H}| = 256$, which means $P(h)$ can be parameterized by a categorical distribution with 256 dimensions. In this analysis, we assume the prior distribution of a mapping is negatively correlated with its coding length α , i.e., $P(h; \alpha, c) \propto 2^{-\frac{\alpha}{c}}$, where c is a normalizing constant to make sure the prior distribution is not too peaky. Usually, the easier-to-learn mappings (i.e., more systematical ones) have higher prior. In Table 3, we demonstrate how to calculate the coding length for the three typical mappings. Note that the mapping that has the highest prior is a degenerate mapping, where $\alpha = 18$ and $P(h) \approx 0.6$. The $P_0(h)$ for all possible mappings are demonstrated in Figure 8.

Table 3: An example of coding the mappings, where α is how many characters (including space and unique symbol, e.g., \rightarrow and $:$) are used to express the grammar.

A systematic mapping $\alpha = 43$		A holistic mapping $\alpha = 56$		A degenerate mapping $\alpha = 18$	
S	\rightarrow z2, z1	S:	00 \rightarrow blue circle	S:	00 \rightarrow Everything
z2:	0 \rightarrow blue	S:	01 \rightarrow red circle		
z2:	1 \rightarrow red	S:	10 \rightarrow red box		
z1:	0 \rightarrow circle	S:	11 \rightarrow blue box		
z1:	1 \rightarrow box				

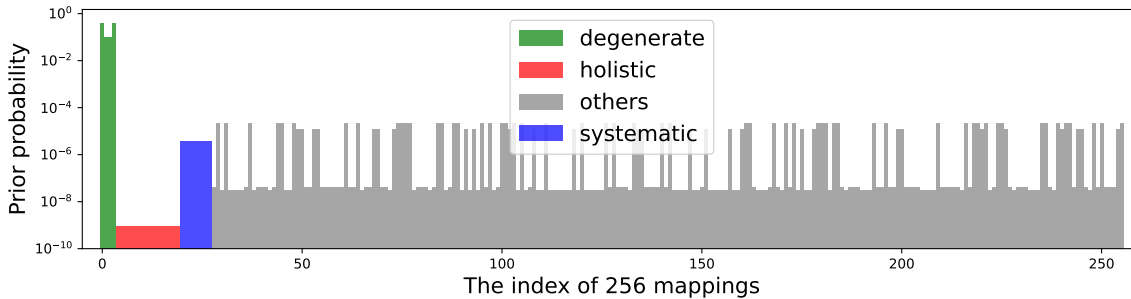


Figure 8: The prior probability of all possible $h \in \mathcal{H}$. The systematic mappings are sandwiched between degenerate and holistic mappings, which means $P_0(h_{degen}) > P_0(h_{sys}) > P_0(h_{holi})$. Some mappings in the “other” group also have relatively large prior, because they contain degenerate components (e.g., mapping two or three objects to the same message).

In this experiment, the knowledge of an agent is encoded in its posterior distribution, i.e., $P_{lm}(h)$. We will observe how this distribution evolves when the agents conduct iterated learning. Recall the sampling behaviors discussed in Section 3. To

get a data sample $d = (x, y)$, we first randomly sample $x \in \mathcal{X}$ from a uniform distribution and then sample y based on the given x ,

$$d \sim P_{lm}(x, y) \propto P_{lm}(y | x) \propto p(y | h, x) \cdot P_{lm}(h). \quad (16)$$

The likelihood $p(y | h, x)$ is defined as:

$$p(y | h, x) = \begin{cases} 1 - \epsilon & \text{if } y \text{ is mapped to } x \text{ in } h \\ \frac{\epsilon}{|\mathcal{Y}| - 1} & \text{otherwise,} \end{cases} \quad (17)$$

where ϵ is a small positive value describing the systematic error during communication.

For the learning behavior, the agent will update the posterior based on the received data samples $\mathbf{d} = (x_i, y_i)_{i=1}^N$:

$$P_{lm}(h) = P(h | \mathbf{d}) \propto p(\mathbf{d} | h) \cdot P_0(h) \propto P_0(h) \cdot \prod_{i=1}^N p(y_i | h, x_i). \quad (18)$$

Now, with the definition of learning and sampling for these Bayesian agents, we can describe how they conduct IL:

- **Initialization:** at the beginning of the t -th generation, a new agent is initialized by $P_0(h)$
- **Imitation:** agent- t learns from \mathbf{d}^{t-1} , which is generated by agent in the previous generation following Equation (18)
- **Interaction:** to impose expressivity pressure, we let agent- t (Alice) play a communication game in this phase. Specifically, we first create another agent Bob by copying $P_{lm}(h)$ from Alice. Then, Alice samples a data pair $d = (x, y)$ on a randomly chosen x and sends it to Bob. Bob will estimate the object based on y . If the estimated $x' = x$, the game succeeds and data pair (x, y) is added to a buffer named \mathbf{d}_{comm} . After several rounds, Alice updates its knowledge by learning from \mathbf{d}_{comm} . Note that in this phase, the pressure of $h \in \mathcal{H}_{\text{eff}}$ is induced implicitly: for the ambiguous h , where multiple x are mapped to the same y , Bob's reconstruction x' might not equal x with high probability. Hence \mathbf{d}_{comm} will finally dominated by the samples generated by those $h \in \mathcal{H}_{\text{eff}}$.
- **Transmission:** after the interaction phase, Alice will generate multiple samples \mathbf{d}^t for the next generation.

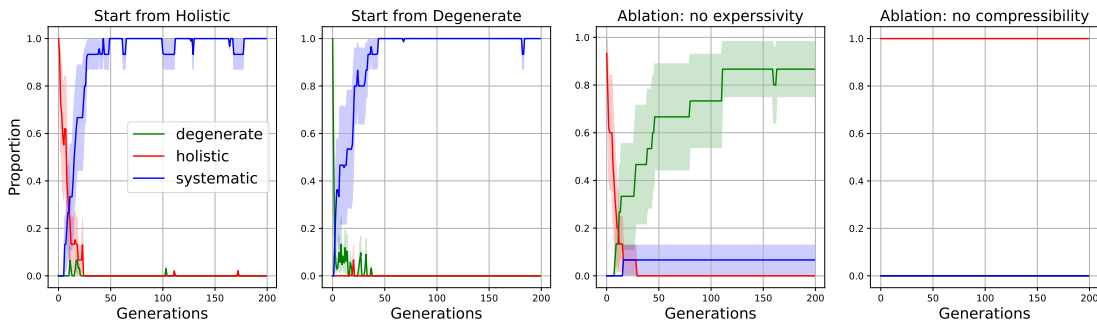


Figure 9: Ratio of three different types of mappings during iterated learning (curves are the average of 15 different runs, shadow region is the variance). Left to right: 1.) \mathbf{d}^0 is a holistic mapping; 2.) \mathbf{d}^0 is a degenerate mapping; 3.) Starting from a holistic \mathbf{d}^0 , but no longer conduct an interaction phase during training. Hence the degenerate language, which has the highest prior, will gradually dominate; 4.) Ablating the compressibility pressure by using a uniform prior distribution.

In the above procedure, the compressibility pressure is embodied in the prior distribution where more reusable principles lead to a higher probability, which aligns with the simplicity bias in the human cognition system. The expressivity pressure is imposed in the communication game because \mathbf{d}_{comm} only contains the unambiguous mappings. Under this setting, we can calculate the weighted proportion (i.e., the summation of the posteriors) of different types of languages and observe how

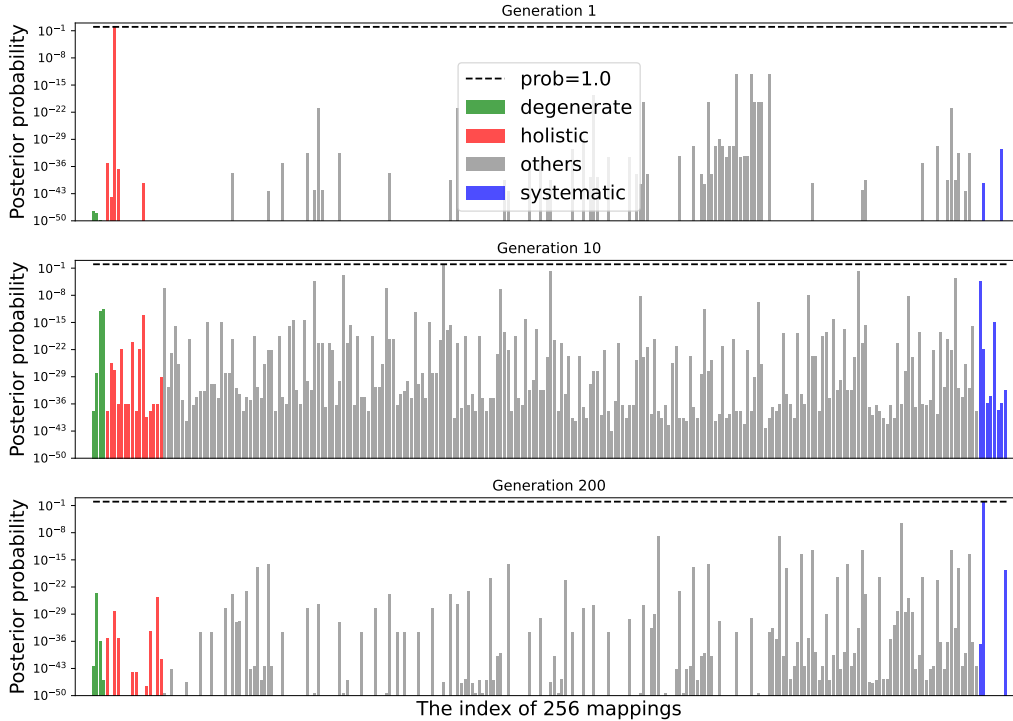


Figure 10: The posterior probabilities of all at the end of different generations.

they evolve during iterated learning, as illustrated in Figure 9. It is clear that the systematic mappings gradually dominate as the learning progresses.

To further verify our theory, we consider a compressibility-only case by removing the interaction phase, and an expressivity-only case using a uniform prior $P(l) = 1/256$. The results in Figure 9 match the theory quite well:

- In an imitation-only iterated learning case, i.e., the third panel in Figure 9, h^T converges to a degenerate mapping, which has the highest prior as illustrated in Figure 8;
- Introducing the interaction phase will rule out those ambiguous mappings (i.e., those $h \notin \mathcal{H}_{\text{eff}}$), and hence h^T converges to systematic mapping, which has the highest prior among all $h \in \mathcal{H}_{\text{eff}}$;
- By comparing the first and second panels in Figure 9, h^T always converges to systematic mapping no matter \mathbf{d}^0 is holistic or degenerate.

Furthermore, we can directly observe the dynamics of $P_{l_m}(h)$ from Figure 10, which provides a more detailed illustration of how the posterior of all mappings changes during training. In the first generation, we see the dominant mapping is a holistic one, which is our \mathbf{d}^0 . Then gradually, under the two pressures, the posterior of systematic mappings gradually increases and finally dominates.

D. More on GPT-based ACRE Experiments

D.1. How to Calculate the Model’s Posterior on All Hypotheses (Figure 11)

Thanks to the instruction-following ability, the GPT can always provide responses following the given format, as illustrated in Figure 11. The experiments demonstrated in this part come from OpenAI’s playground. The model we use is `gpt-3.5-turbo-instruct`. The temperature is 0.1 and the probability feedback is enabled. We let the model return probabilities of the top 5 candidate tokens for each token in the response, as illustrated by the three sub-panels in the figure. Then, the posterior of specific h can be calculated by multiplying the probability of all tokens

with corresponding values. For example, $P_{lmw}(h = \{A: \text{on}, B: \text{und}, C: \text{off}, D: \dots\})$ can be calculated by $P(r_5 = \text{on}) \cdot P(r_9 = \text{und}) \cdot P(r_{13} = \text{off}) \dots$, where $r_{5,9,13,\dots}$ are the tokens denoting the corresponding values of A, B, C . To further show the feasibility of this approach, we conduct the following two verifications. First, we calculate $\prod_{i \in \mathcal{I}_{\text{format}}} P(r_i)$ and find that this value is always close to one ($\mathcal{I}_{\text{format}}$ denotes the indexes of those format-related tokens, e.g., `Rule`, `{`, `:`, `A`, `B`, `C`, etc). This means the model reliably follows the instructions when generating responses. Second, we calculate $P_{lmw}(h)$ for all possible 243 different h and verified that $\sum_{h \in \mathcal{H}} P_{lmw}(h)$ is always close to one.

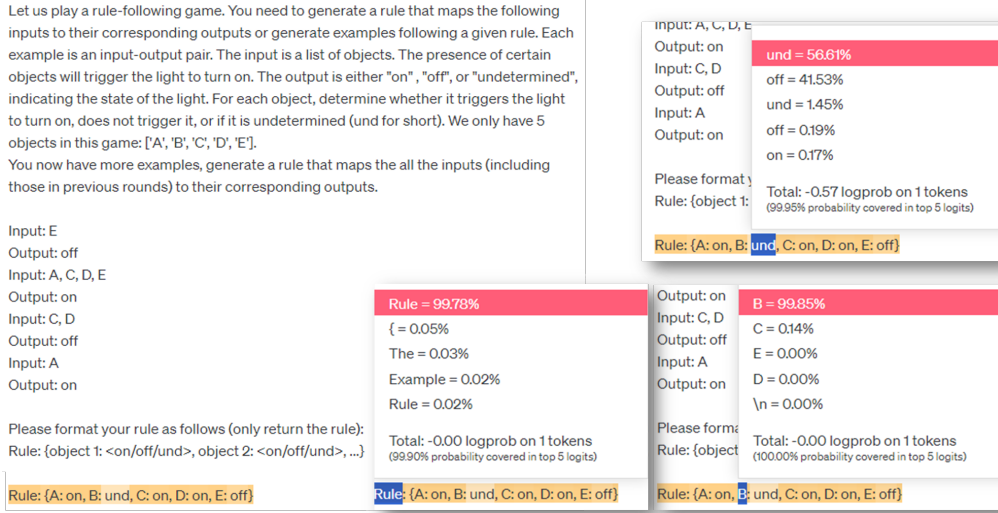


Figure 11: How GPT provides the rule following the given format, which makes it possible to calculate $P_{lmw}(h)$ for all h .

D.2. How to Control the Bias in the Prior

We demonstrate how to manipulate bias in the prior $P_0(h)$ in the ACRE task by adding spurious correlations in the prompt and by changing the name of the object. The prompt we use is almost the same as that in Figure 11. We will analyze the value of $P(r_{20})$, i.e., the probability of the token denoting the status of the last object in the rule. The \mathbf{d}^0 in these experiments are all the same (i.e., $[B, D] \rightarrow \text{on}$; $[B, C] \rightarrow \text{und}$; $[B, D, E] \rightarrow \text{on}$, as stated in the last several panels in Figure 12). Some subtle modifications under different settings will be described one by one in the following:

- ①: the default setting, where the object list is $[A, B, C, D, E]$. The $P_0(r_{20} = [\text{on}, \text{off}, \text{und}])$ are $[11.8\%, 6.46\%, 81.68\%]$. This makes sense, as all these 3 statuses of E can describe all examples in \mathbf{d}^0
- ①: compared with ①, we change the object E to `screen`, and no extra text is added to the prompt. Then, as the screen is likely to be turned on during the experiment, $P_0(r_{20} = \text{on})$ dominates the prediction;
- ②: compared with ①, we add a sentence “Turn off the screen after the experiment” to the task instruction. This misleading sentence introduces a bias towards `screen:off` by creating a spurious correlation;
- ③: compared with ②, we use a synonym “close the screen” to replace the “turn off the screen” in the prompt. As the word “off” does not exist in the prompt, the bias towards `screen:off` is weakened;
- ④: compared with ②, we change the name `screen` to `Sony screen` in the example, but left the prompt unchanged. We see the model is clever enough to distinguish which screen we refer to, and hence keeps the preference of $P_0(r_{20})$ demonstrated in ①;
- ⑤: here we change the object to another name `John`, which also keeps the preference of $P_0(r_{20})$ demonstrated in ①;
- ⑥: compared with ⑤, we add the sentence “John will turn off the screen after experiment”. Then we find the bias towards `John:off` is slightly increased, but not as strong as that in ②, which provides us another way to control the strength of the bias;

⑦: in the following three cases, we put the position of the misleading sentence before the examples \mathbf{d}^0 . Compared with ②, the bias towards `screen:off` is significantly amplified. This might be because the attention mechanism lets the model recite the fact that the screen is off before reading the examples (remember that `screen:off` also explains all examples);

⑧: compared with ④, where the object is also Sony `screen`. Here the bias is stronger than ④ but weaker than ⑦, which verifies that adding spurious correlation before examples can amplify the bias while modifying the object name can reduce the bias;

⑨: compared with ③, which also uses the synonym in the prompt, the bias becomes stronger.

In summary, we have several principles when controlling the strength of the bias in $P_0(h)$:

- Adding spurious correlation before \mathbf{d}^0 provide very strong bias;
- Using synonyms rather than phrases containing specific states (e.g., close/open v.s. turn off/on) weakens the bias;
- Using two slightly different object names (i.e., Sony screen v.s. screen) weakens the bias;
- Using indirect spurious correlation (e.g., John v.s. screen) weakens the bias.



Figure 12: An example of how to manipulate $P_0(h)$ by adding spurious correlation in the prompt. The task instruction is the same as that provided in Figure 11, except the object name (in the blue box) and the added hints (in the red box).

For the experiments in Figure 14 and Figure 3, the six different levels of prior bias are controlled by the following prompts:

- Very high: add “Turn off the screen after the experiment.” before and after \mathbf{d}^t is given;
- High: add “Turn off the screen after the experiment.” before \mathbf{d}^t ;
- Medium: add “Turn off the screen of the monitor after the experiment.” before \mathbf{d}^t ;
- Mild: add “John will turn off the screen after the experiment.” before \mathbf{d}^t ;
- Low: add “Close the screen after the experiment.” before \mathbf{d}^t ;
- Very low: add “Close the screen after the experiment.” after \mathbf{d}^t ;

D.3. The Prompt Design for ACRE Task (Figures 15 to 17)

Please also refer to the three figures and the `log.txt` file in our code base.

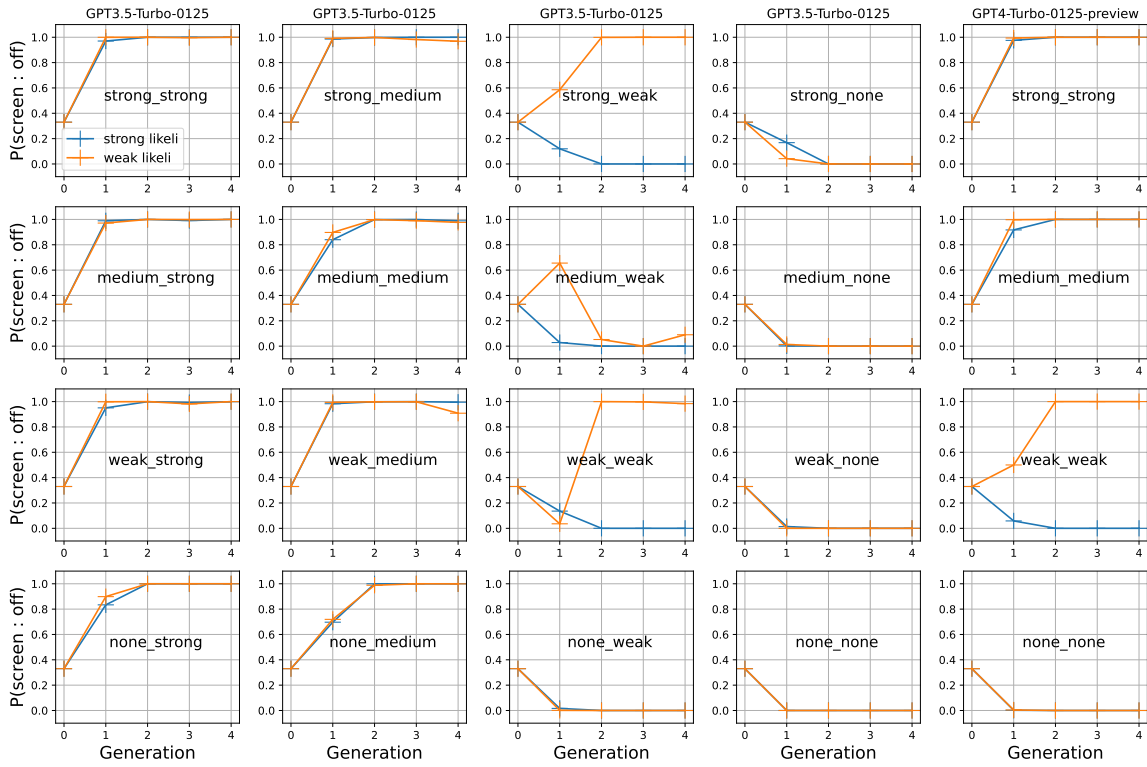


Figure 13: A more detailed analysis of the competition between the likelihood $p(\mathbf{d} | h)$ and bias in $P_0(h)$. The first 4 columns are results from the new GPT3.5 and the last column is from GPT4. In each panel, the two curves represent strong and weak likelihood cases, which are controlled by the ground truth h^* . The h^* in strong cases contains 3 objects being "on" while the weak cases only have 1. The text in each panel represents the level of spurious correlation we introduce before and after \mathbf{d} by manipulating the instruction prompt. For example, `strong_strong` means we put strong bias, i.e., "Turn off the screen after experiments", before and after \mathbf{d}^t in each generation. The trend of these panels aligns well with our previous results and analysis.

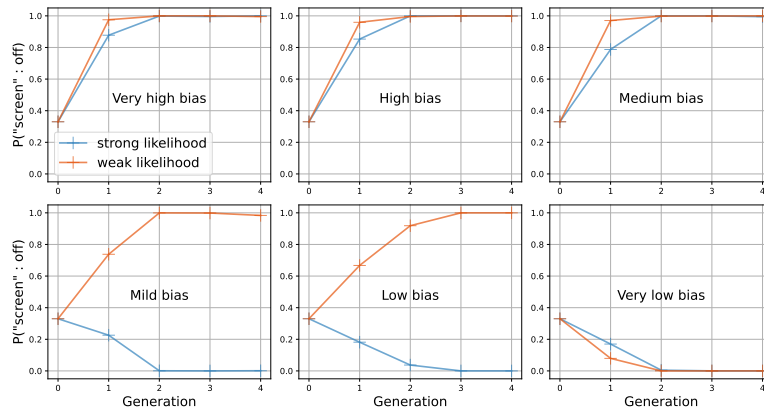


Figure 14: The follow-up experiments of the one mentioned in Figure 3. In this figure, we put curves of the same level of prior bias (but with different likelihoods) in the same panel. It is clear that in most cases, the stronger likelihood will weaken the influence of the bias (that is why the orange curve is above the blue curve).

System:

Let us play a rule following game. You need to generate a rule that maps the following inputs to their corresponding outputs, or generate examples following a given rule. Each example is an input-output pair. The input is a list of objects. If any objects with status on in the input, the output should be on. If all objects in the input are off, the output is off. If only objects with off and und in the list, the output should be undetermined (und for short). The output is either "on", "off", or "und", indicating the state of the light. For each object, determine whether it triggers the light to turn on, does not trigger it, or if it is undetermined. We only have 5 objects in this game: ['A', 'B', 'C', 'D', 'E'].

Gen1 - user:

You now have more examples, generate a rule that maps all the inputs (including those in previous rounds) to their corresponding outputs.

Input: A
Output: und
Input: B, D
Output: on
Input: A, C
Output: und
Input: B, D, E
Output: on

$$d^0 \sim p(d|h^*)$$

Please format your rule in the following format.
Rule: {"object 1": <"on"/"off"/"und">, "object 2": <"on"/"off"/"und">, ...}

Gen1 - assistant:

Rule: {"A": "und", "B": "on", "C": "und", "D": "on", "E": "on"}

$$h^1 \sim P_{lm}(h|d^0)$$

Gen1 - user:

The rule you provided is {"A": "und", "B": "on", "C": "und", "D": "on", "E": "on"}. Based on this rule, can you give 4 examples with different inputs those are unseen before? Remember the input is a list of objects. If any objects with status on in the input, the output should be on. If all objects in the input are off, the output is off. If only objects with off and und in the list, the output should be undetermined (und for short).

Gen1 - assistant:

Input: A, B, C, D, E
Output: on
Input: A, B, C
Output: und
Input: A, B, D
Output: on
Input: B, E
Output: on

$$d^1 \sim P_{lm}(d|h^1)$$

Gen2 - assistant:

You now have more examples, generate a rule that maps all the inputs (including those in previous rounds) to their corresponding outputs.

Input: A, B, C, D, E
Output: on
Input: A, B, C
Output: und
Input: A, B, D
Output: on
Input: B, E
Output: on

Please format your rule in the following format.
Rule: {"object 1": <"on"/"off"/"und">, "object 2": <"on"/"off"/"und">, ...}

Figure 15: Prompt design and an example dialogue for the imitation-only iterated learning on the ACRE dataset. The shaded region and arrows represent that we copy specific text to form the message. The messages starting with the role of **system** and **user** are sent to GPT, while those starting with **assistant** are the feedback from GPT. For this multi-round chat, we will feed all historical information to API, see our code for more details.

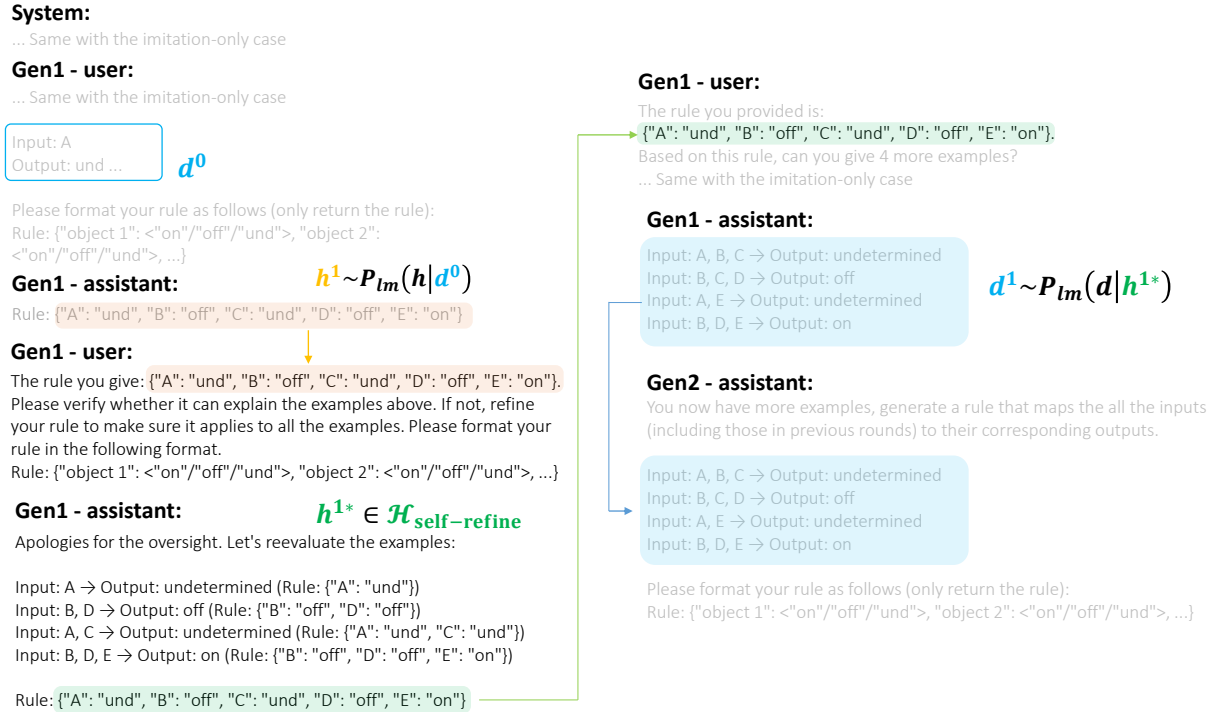


Figure 16: Prompt design for iterated learning with self-refine (Madaan et al., 2023) as the interaction phase. The text in gray is the same as the default imitation-only setting. Note that the format of the examples might be changed (like the examples in Gen-1: assistant), which doesn't influence the experimental results.

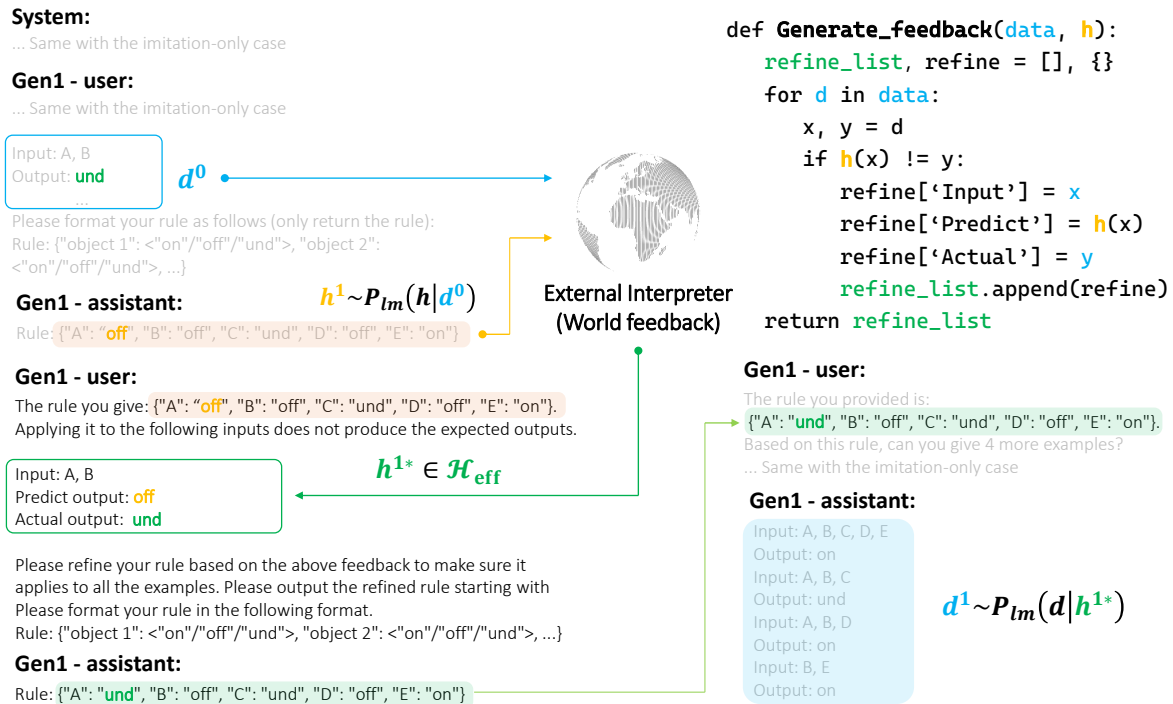


Figure 17: Prompt design for iterated learning with hypothesis search (Qiu et al., 2024) as the interaction phase. Compared with self-refine, it introduces an external interpreter to refine h proposed by the model, where \mathcal{H}_{eff} is the ground-truth one.

E. More on Self-data-augmentation Task (Table 4 and 5; Figure 18, 19, and 20)

In this appendix, we first introduce the prompt design of the experiment on both imitation-only settings, as well as the experiments with five different \mathcal{H}_{eff} . Please refer to Figure 18 for more details.

Then, we provide the full results of the experiment in Table 4, 5 and Figure 19, from which we can derive more interesting findings. In general, the figure demonstrates how different metrics evolve for different generations while the table reports the converged values at the last generation.

From the first column in this figure, we observe that other than the $\mathcal{H}_{\text{hard}}$ setting, all curves in other settings show a clear trend of convergence towards the top of the figures. This means iterative learning indeed amplifies the hidden bias of $P_0(h_{\text{easy}}) > P_0(h_{\text{hard}})$ when the imposed \mathcal{H}_{eff} doesn't impede this bias. In the $\mathcal{H}_{\text{random}}$ setting, the $\hat{\mathbf{d}}$ is sampled from all the data generated by the previous generation, which makes those hard samples more likely to be sampled compared with the imitation-only settings or those with $\mathcal{H}_{\text{easy/long/short}}$. Hence we observe the converging speed of it is slightly lower than these settings. On the contrary, when $\mathcal{H}_{\text{hard}}$ is introduced, the bias towards h_{easy} is successfully restrained. We observe a clear competition between these two pressures: the curve first goes up, which means the bias towards easy samples is stronger. However, as the learning goes on, the curves turn down again as we later have more hard samples in $\mathcal{D}_{\text{pool}}$.

The second column of the figure demonstrates the average ranking of words in \mathbf{d}^t . We observe a similar trend in the ratio of easy samples, although our \mathcal{H}_{eff} never explicitly constrains it. **This phenomenon hints to us that when conducting an iterative self-data-augmentation algorithm, some unknown bias would be implicitly amplified although we already designed another \mathcal{H}_{eff} for other properties.** Imagine we are conducting the ReST algorithm (Gulcehre et al., 2023). We can pursue the correctness of \mathbf{d}^t by ranking all examples by training a reward model that prefers more correct responses. However, some other subtle biases, like conciseness, informativeness, etc., might be ignored by the algorithm designer and are hence unexpectedly amplified. In summary, we should bear in mind that identifying the good and bad bias in $P_0(h)$ is quite important for an appropriate evolution.

Finally, we use the last column and the average length of the acronym to show how to make a composed \mathcal{H}_{eff} by combining more than one attribute of the data. It is clear that both $\mathcal{H}_{\text{easy/long}}$ and $\mathcal{H}_{\text{easy/short}}$ did their jobs quite well: the converged \mathbf{d}^6 contains the samples with desired properties as we expected. Another thing that heavily influences the results is the ratio of easy examples in \mathbf{d}^0 . Although the theory claims that the converged results are irrespective of \mathbf{d}^0 , the converging speed and the difficulty of amplifying specific bias heavily depends on \mathbf{d}^0 . This claim can be well supported by the fact that when N_e is small, amplifying the bias of h_{easy} is significantly harder than the large N_e case.

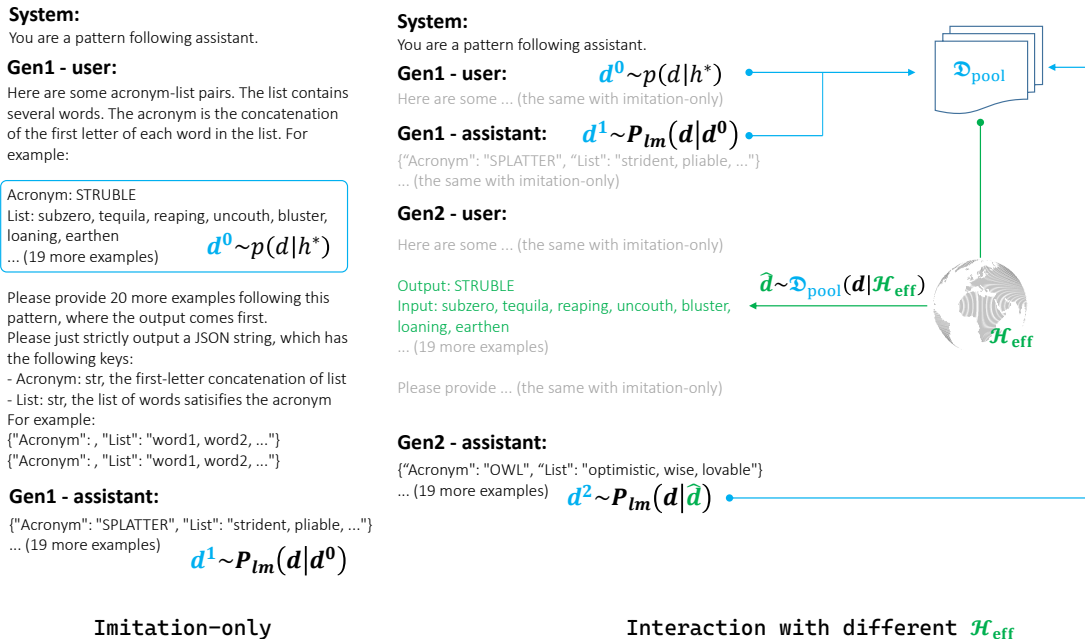


Figure 18: Prompt design for iterated learning on the acronym data-generation task.

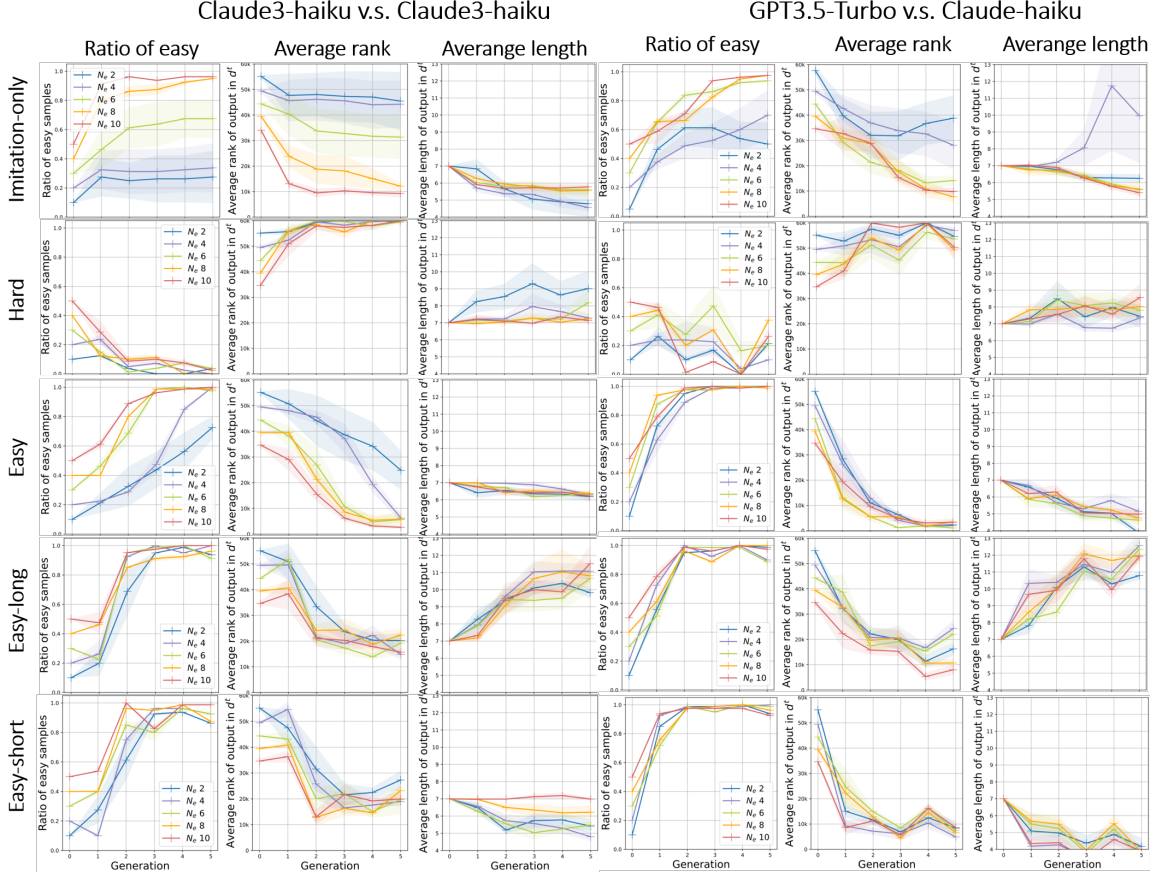


Figure 19: Results when adding different interaction phases (4 different seeds). Combined with Figure 5, all the three settings (i.e., old GPT 3.5 plays with old GPT; Claude plays with Claude, and new GPT plays with Claude) demonstrate similar evolutionary trends, which match our theory quite well.

Table 4: Claude3-haiku results under different \mathcal{H}_{eff} . We color the highest and lowest numbers in each column differently.

Ne=	Ratio-easy					Avg-rank					Avg-length				
	2	4	6	8	10	2	4	6	8	10	2	4	6	8	10
Imitation-only	0.275±0.18	0.338±0.17	0.675±0.13	0.950±0.00	0.962±0.00	45477	44235	31356	12148	9272	4.788±2.21	4.563±0.14	5.613±0.46	5.563±0.15	5.775±0.05
Hard	0.036±0.00	0.000±0.00	0.038±0.00	0.000±0.00	0.025±0.00	59484	60001	59458	60001	59874	9.014±4.32	7.288±0.20	8.175±2.89	7.238±0.11	7.137±0.12
Easy	0.725±0.08	1.000±0.00	0.975±0.00	0.988±0.00	1.000±0.00	24809	6233	5644	5827	2646	6.188±0.25	6.300±0.04	6.338±0.09	6.375±0.07	6.225±0.22
Easylong	0.938±0.00	1.000±0.00	0.913±0.02	0.963±0.00	1.000±0.00	20208	14803	19200	22333	15708	9.825±0.37	11.077±0.82	10.650±2.47	10.813±1.41	11.513±3.97
Easysort	0.863±0.00	0.925±0.00	0.925±0.02	0.875±0.00	0.988±0.00	27286	19021	19749	23155	19979	5.413±0.60	4.800±0.14	5.475±0.23	6.225±0.68	6.988±0.01

Table 5: GPT3.5-Turbo 0125 plays with Claude3-haiku results when adding different \mathcal{H}_{eff} .

Ne=	Ratio-easy					Avg-rank					Avg-length				
	2	4	6	8	10	2	4	6	8	10	2	4	6	8	10
Imitation-only	0.363±0.11	0.575±0.14	0.975±0.00	1.000±0.00	0.975±0.00	44334	33977	10960	6398	9688	6.363±0.39	7.705±5.25	4.475±0.26	5.134±0.20	5.012±0.22
Hard	0.000±0.00	0.025±0.00	0.110±0.01	0.000±0.00	0.000±0.00	60001	59382	57022	60001	60001	8.225±2.76	6.700±0.27	8.606±0.90	7.950±0.69	8.063±1.18
Easy	1.000±0.00	1.000±0.00	1.000±0.00	1.000±0.00	1.000±0.00	777	1552	1341	1048	1850	4.750±0.11	5.350±0.53	5.175±0.19	4.888±0.07	4.975±0.32
Easylong	0.988±0.00	1.000±0.00	1.000±0.00	1.000±0.00	1.000±0.00	15967	10009	9087	7432	6146	11.025±0.54	10.86±0.52	10.525±1.99	11.975±2.03	10.875±0.59
Easysort	0.975±0.00	1.000±0.00	1.000±0.00	0.913±0.02	1.000±0.00	14139	7848	15015	16249	12356	4.163±0.90	3.213±0.12	3.513±0.22	3.825±0.09	3.887±0.45

1. {"Acronym": "ASTROPH", "List": "astronomer, physicist, hypothesis, yearn, spectrum, photon, youth"}	{"Acronym": "anemone", "List": "apple, blueberry, cherry, daisy, elderberry, fig, grape"}
2. {"Acronym": "BIOCHEM", "List": "bacteria, investigate, occupy, chemistry, host, emulate, mutate"}	{"Acronym": "banana", "List": "banana, cherry, dahlia, elderberry, fig, grape, kiwi"}
3. {"Acronym": "CHRONIC", "List": "children, hear, restless, occupy, night, investigate, create"}	{"Acronym": "cherry", "List": "cherry, daisy, elder, fig, grape, hyacinth, iris"}
4. {"Acronym": "DATASETS", "List": "data, analyze, test, establish, samples, tabulate, sort"}	{"Acronym": "dahlia", "List": "dahlia, elder, fig, geranium, hyacinth, iris, jasmine"}
5. {"Acronym": "ELECTRIC", "List": "element, light, energy, convert, transmit, efficiency, control"}	{"Acronym": "elder", "List": "elder, fig, geranium, hyacinth, iris, jasmine, kiwi"}
6. {"Acronym": "FISHERY", "List": "fin, isolate, spawn, hatch, eggs, reproduce, young"}	{"Acronym": "fig", "List": "fig, geranium, hyacinth, iris, jasmine, kangaroo, kiwi"}
7. {"Acronym": "GEOLOGIC", "List": "geology, erosion, observe, lithosphere, oceanic, crust, investigate"}	{"Acronym": "geranium", "List": "geranium, hyacinth, iris, jasmine, kangaroo, kiwi, lemon"}
8. {"Acronym": "HELIOSPH", "List": "heliosphere, electromagnetic, lunar, ionized, solar, plasma, hydrogen"}	{"Acronym": "grape", "List": "grape, hyacinth, iris, jasmine, kangaroo, kiwi, lily"}
9. {"Acronym": "INTERNET", "List": "interface, network, transfer, encode, routing, encryption, transmit"}	{"Acronym": "hyacinth", "List": "hyacinth, iris, jasmine, kangaroo, kiwi, lily, mango"}
10. {"Acronym": "JOURNALS", "List": "journal, observe, judge, record, notes, summarize, share"}	{"Acronym": "iris", "List": "iris, jasmine, kangaroo, kiwi, lily, mango, nectarine"}
11. {"Acronym": "KINDERG", "List": "kindergarten, introduce, nurture, develop, grow, encourage, love"}	{"Acronym": "jasmine", "List": "jasmine, kangaroo, kiwi, lily, mango, nectarine, orange"}
12. {"Acronym": "LABORAT", "List": "laboratory, analyze, biology, observe, research, technology, apparatus"}	{"Acronym": "kiwi", "List": "kiwi, lily, mango, nectarine, orange, pear, peony"}
13. {"Acronym": "MANAGEMENT", "List": "manage, administer, negotiate, goals, execute, monitor, take, action"}	{"Acronym": "lily", "List": "lily, mango, nectarine, orange, pear, peony, quince"}
14. {"Acronym": "NEUROSCI", "List": "neuron, excitation, understanding, regeneration, organization, synapses, interactions"}	{"Acronym": "mango", "List": "mango, nectarine, orange, pear, peony, quince, rose"}
15. {"Acronym": "OPTIONAL", "List": "open, prefer, observe, take, proposals, interests, actions, learn"}	{"Acronym": "nectarine", "List": "nectarine, orange, pear, peony, quince, rose, strawberry"}
16. {"Acronym": "POLITICS", "List": "population, order, law, identify, territorial, organization, conflicts, solve"}	{"Acronym": "orange", "List": "orange, pear, peony, quince, rose, strawberry, tangerine"}
17. {"Acronym": "QUANTITY", "List": "quality, understand, quantify, analyze, theory, numerically, verify"}	{"Acronym": "peony", "List": "peony, quince, rose, strawberry, tangerine, tulip, violet"}
18. {"Acronym": "RESEARCH", "List": "review, essential, studies, evaluate, consider, hypothesis, research, design"}	{"Acronym": "quince", "List": "quince, rose, strawberry, tangerine, tulip, violet, watermelon"}
19. {"Acronym": "SOFTWARE", "List": "source, open, organize, write, programs, format, execute, review"}	{"Acronym": "rose", "List": "rose, strawberry, tangerine, tulip, violet, watermelon, xenon"}
20. {"Acronym": "TOXICITY", "List": "toxic, understand, oxidation, identify, complex, systems, interaction, you"}	{"Acronym": "strawberry", "List": "strawberry, tangerine, tulip, violet, watermelon, xenon, yellow"}
	{"Acronym": "tulip", "List": "tulip, violet, watermelon, xenon, yellow, zinnia, zucchini"}
	{"Acronym": "violet", "List": "violet, watermelon, xenon, yellow, zinnia, zucchini, apple"}
	{"Acronym": "watermelon", "List": "watermelon, xenon, yellow, zinnia, apple, banana, cherry"}
	{"Acronym": "xenon", "List": "xenon, yellow, zinnia, apple, banana, cherry, elderberry"}
	{"Acronym": "yellow", "List": "yellow, zinnia, apple, banana, cherry, elderberry, fig"}
	{"Acronym": "zinnia", "List": "zinnia, apple, banana, cherry, elderberry, fig, grape"}

Typical examples generated by Mixtral-8x7b (left) and Mixtral-7b (right). Compared with GPT and Claude, Mixtral tend to provide examples in an alphabet order. Mixtral-7b usually violate the instructions (e.g., list not match acronym, generate more than 20 examples, etc).

Figure 20: An interesting observation of Mixtral series models: they have a bias toward alphabet examples. However, as the Mixtral model usually has typos in their response (like the right panel), we do not have the full results of these models.